Elevated intracellular cAMP concentration mediates growth suppression in glioma cells

Dewi Safitri[1,2], Matthew Harris[1], Harriet Potter[1], Ho Yan Yeung[1], Ian Winfield[1], Liliya Kopanitsa[3], Fredrik Svensson[3,4], Taufiq Rahman[1], Matthew T Harper[1], David Bailey[3], Graham Ladds[1,*].

[1] *Department of Pharmacology, University of Cambridge, Tennis Court Road, Cambridge CB2 1PD, United Kingdom*

[2] *Pharmacology and Clinical Pharmacy Research Group, School of Pharmacy, Bandung Institute of Technology, Bandung 40132, Indonesia*

[3] *IOTA Pharmaceuticals Ltd, Cambridge University Biomedical Innovation Hub, Clifford Allbutt Building, Hills Road, Cambridge CB2 0AH, United Kingdom*

[4] *Computational Medicinal Chemistry, Alzheimer's Research UK UCL Drug Discovery Institute, The Cruciform Building, Gower Street, London, WC1E 6BT*

*Corresponding author: Dr Graham Ladds, Department of Pharmacology, University of Cambridge, Tennis Court Road, Cambridge, CB2 1PD Tel; +44 (0) 1223 334020. Email: grl30@cam.ac.uk.

ABSTRACT

Supressed levels of intracellular cAMP have been associated with malignancy. Thus, elevating cAMP through activation of adenylyl cyclase (AC) or by inhibition of phosphodiesterase (PDE) may be therapeutically beneficial. Here, we demonstrate that elevated cAMP levels suppress growth in C6 cells (a model of glioma) through treatment with forskolin, an AC activator, or a range of small molecule PDE inhibitors

with differing selectivity profiles. Forskolin suppressed cell growth in a PKA-dependent manner by inducing a G_2/M phase cell cycle arrest. In contrast, trequinsin (a non-selective PDE2/3/7 inhibitor), not only inhibited cell growth via PKA, but also stimulated (independent of PKA) caspase-3/-7 and induced an aneuploidy phenotype. Interestingly, a cocktail of individual PDE 2,3,7 inhibitors suppressed cell growth in a manner analogous to forskolin but not trequinsin. Finally, we demonstrate that concomitant targeting of both AC and PDEs synergistically elevated intracellular cAMP levels thereby potentiating their antiproliferative actions.

Keywords: cAMP, phosphodiesterase inhibitors, proliferation, glioma, caspase, cell cycle

1. INTRODUCTION

Glioma is a general term for brain tumours that originate from glial cells in the central nervous system and which may progressively lead to death if not treated early [1, 2], with glioblastoma, the most common type of glioma, showing particularly poor survival [3]. The development of novel therapeutic approaches targeting glioma and glioblastoma are urgently required.

Defects in a number of signalling pathways have been reported in glioma pathogenesis, including the phosphatidylinositol-3 kinases/ phosphatase and tensin/ protein kinase B/ mammalian target of rapamycin (PI3K/PTEN/Akt/mTOR) cascade; the retinoblastoma pathway (pRB); the Ras/ mitogen-activated protein kinase (RAS/MAPK) pathway; signal transducer and activator of transcription 3 (STAT3); zinc transporter 4 (ZIP4); as well as the adenylyl cyclase (AC) system [4].

Importantly, lower cAMP levels are observed in brain tumour tissue (25.8 pmol/mg protein) compared to normal healthy tissue (98.8 pmol/mg protein) [5]. Indeed forskolin, an AC activator that elevates cAMP levels, has shown promising results in ameliorating cancer development [6]. While high levels of intracellular cAMP may kill cancer cells, the exact molecular mechanisms have not been clearly elucidated. Direct elevation of cAMP using the cAMP analogues 8-bromo-cAMP, 8-chloro-cAMP, monobutyryl cAMP and dibutyryl cAMP, however, cannot be recommended due to the toxicity of these compounds [7]. Thus, there is a need to develop safe and effective compounds that can increase cAMP levels by pharmacological intervention.

Depending on the cell type where the malfunctions are observed, cAMP may play a role in either promoting or suppressing cell proliferation. This incongruity can be explained by two theories on the cAMP signalling cascade. The first theory proposes that elevation of intracellular cAMP is beneficial for suppressing cell proliferation in most mesenchymal and epithelial cell lines, such as glioblastoma [8], thyroid cells [9], ovarian granulosa cells [10], fibroblasts [11], and primary cardiomyocytes [12]. In contrast, the second theory proposes that cAMP promotes cell survival, which has been observed in myeloid cells, pancreatic β-cells, hepatocytes, gastric and intestinal cells, spinal motor, superior cervical ganglion sympathetic, dorsal root ganglion, dopaminergic neurons, cerebral granule and septal cholinergic neurons [13]. These two divergent roles of cAMP may be crucial in both physiological maintenance and pathological conditions, but whether these signalling cascades are interconnected remains unclear.

It has been well established that after synthesis by AC activation, cAMP diffuses within cells and is hydrolyzed to 5'AMP by phosphodiesterases (PDEs). PDEs are a

subfamily of ectonucleotidases consisting of 11 isoforms (PDE1–11) in mammals and are encoded by 21 different genes [14], which are distributed in many types of tissue [15]. Each isoenzyme possesses different affinities for cAMP and/or cGMP, kinetic characteristics, allosteric regulation by cAMP/cGMP and, phosphorylative control by various protein kinases, that result in their distinctive response to a stimulus [16, 17]. To date, there are 3 classes of PDEs subdivided according to their substrate specificities: cAMP-specific PDEs (PDE4, PDE7 and PDE8), cGMP-specific PDEs (PDE5, PDE6 and PDE9), and dual-substrate PDEs (PDE1, PDE2, PDE3, PDE10 and PDE11) [18]. Through metabolizing both cAMP and cGMP, PDEs generate intracellular gradients and microdomains of these second messengers to regulate their spatio-temporal signalling [19]. PDEs prevent non-specific activation, enabling both specificity and selectivity towards intracellular targets [20].

Overexpression of some PDEs, such as PDE1, PDE4, PDE5, and PDE7, has been reported to alter patterns of cAMP in the brain [21-24]. Some evidence shows that particular PDE inhibitors, such as rolipram, a selective PDE4 inhibitor, prevents leukaemia proliferation through an elevation of cAMP and an induction of apoptosis. This suggests that using specific PDE inhibitors is a viable approach for cancer therapy [25]. Given that PDE inhibitors may offer therapeutic efficacy against cancer, we investigated the role of each PDE upon cAMP accumulation and cell proliferation in a glioma cell model using a range of pharmacological inhibitors. Our data indicates that tumour cell regression is linearly correlated with elevation of cAMP. Among all PDE inhibitors tested, trequinsin (a non-selective PDE2/3/7 inhibitor [26]) was found to be the most potent at inhibiting cell proliferation. More importantly, by using small molecule compounds we highlight that simultaneous elevation of cAMP through activation of AC and inhibition of multiple PDEs (specifically PDE2, PDE3 and PDE7)

had synergistic anti-proliferative effects on the glioma cells, predominantly by altering cell cycle progression and inducing activation of caspase-3/7, providing a novel treatment strategy for glioma.

2. MATERIALS AND METHODS

2.1 Cell Lines

C6 glioma cells (a gift from Prof. Colin Taylor, University of Cambridge) were cultured in Gibco® Minimum Essential Medium (Thermo Fisher Scientific, UK) supplemented with 10% foetal bovine serum (FBS, Sigma, UK), 2 mM L-glutamine (Sigma, UK), and 1% antibiotic/antimycotic (Sigma, UK). ST14A cells (rat-derived striatal cells (Tissue and Cell Biotechnologies, Italy) were grown in Gibco® DMEM/F12 1:1 (1X) – Glutamax TM (Thermo Fisher Scientific, UK), supplemented with 10% FBS and 1% antibiotic/antimycotic. C6 cells were maintained at 37 °C in humidified 95% air and 5% CO_2. ST14A cells were grown at 33 °C in humidified 95% air and 5% CO_2 because propagation of ST14A cells at 37 °C has been shown to induce differentiation into glial cells [27]. Where appropriate cells were treated with pertussis toxin (PTX, Thermo Fisher, UK) at a range concentration of 2 pg/ml to 200 ng/ml or cholera toxin (CTX, Sigma, UK), at a concentration of 3.5 pg/ml to 350 ng/ml. PTX uncouples receptor-mediated $G\alpha_i$-dependent inhibition of cAMP production, meanwhile CTX inhibits GTPase activity of $G\alpha_s$ and causes permanent activation [28, 29].

2.2 Compounds

Forskolin (Sigma, UK) was diluted to a stock of 100 mM in DMSO (Sigma, UK). Cholera toxin (CTX) was diluted in water to a stock of 35 µg/ml, whereas pertussis toxin (PTX) was diluted at a stock of 100 µg/ml. Isoprenaline hydrochloride (Sigma,

UK) was dissolved in water to a stock of 10 mM. Trequinsin, PF-2545920, vinpocetine, sildenafil, rolipram, cilostamide, caffeine, SQ22536, EHNA, amrinone, zaprinast, TC3.6, ibudilast, milrinone, BAY 73-6691, BRL-50481, piclamilast, IBMX, roflumilast, tadalafil, PF-04449613 (all purchased from Sigma, UK), BC 11-38, and PF 04671536 (both obtained from Tocris, UK) were dissolved in DMSO to stock concentrations of either 100 mM or 10 mM. Guanylyl cyclase activators BAY 41-8543 and YC-1 were purchased from Tocris and diluted to a stock of 100 mM in DMSO. Exchange protein directly regulated by cAMP (Epac) inhibitors ESI-09, HJC0350, and CE3F4 (all purchased from Sigma, UK) were diluted to 10 mM stocks in DMSO. Protein kinase A (PKA) and protein kinase G (PKG) inhibitors, KT5720 and KT5823, respectively (all obtained from Cambridge Insight Biotechnology, UK) were diluted to stocks of 100 mM and 1 mM, respectively. MRP4 (multidrug resistant protein 4) inhibitor, PU23 (Tocris, UK), was dissolved in DMSO to a stock of 50 mM.

2.3 Reverse Transcription PCR

RNA was extracted from C6 and ST14A cells using RNAqueous®-4PCR Total RNA Isolation Kit (Life Technologies, UK) according to manufacturer's instructions. In order to remove any contamination of genomic DNA, all RNA samples were treated with DNAse I included in the kit. The purity of RNA samples was quantified using a NanoDrop^{TM} Lite spectrophotometer (Thermo Scientific, UK) and only samples that had a minimum yield of 100 ng/μL and $A_{260/280}$ >1.9 were used in the experiments. Complementary DNA was synthesized using a QuantiTect reverse transcription kit (Qiagen, UK). The oligonucleotides (Sigma, UK) used for PCR were designed specifically for rat, including *GAPDH*: forward 5′-TCCCTCAAGATTGTCAGCAA-3′, reverse 5′- AGATCCACAACGGATACATT-3′ (309 bp); *PDE1A*: forward 5′-

CGCCTGAAAGGAATACTAAGA-3′, reverse 5′-TAGAAGCCAACCAGTCCCGGA-3′ (211 bp); *PDE1B*: forward 5′- CTGTCACCCCGCAGTCCTCCG-3′, reverse 5′-GAAGGTGGAGGCCAGCCAGTC-3′ (309/306 bp); *PDE1C* forward 5′-CGCGGGCTGAGGAAATATAAG-3′, reverse 5′-GAAGGTGGAGGCCAGCCAGTC-3′ (237 bp); *PDE2A*: forward 5′-CCAAATCAGGGACCTCATATTCC-3′, reverse 5′-GGTGTCCCACAAGTTCACCAT-3′ (86 bp); *PDE3A*: forward 5′-CACAAGCCCAGAGTGAACC-3′, reverse 5′-TGGAGGCAAACTTCTTCTCAG-3′ (123 bp); *PDE3B*: forward 5′-GTCGTTGCCTTGTATTTCTCG-3′, reverse 5′-AACTCCATTTCCACCTCCAGA-3′ (103 bp); *PDE4A*: forward 5′-CGACAAGCACACAGCCTCT-3′, reverse 5′-CTCCCACAATGGATGAACAAT-3′ (73 bp); *PDE4B*: forward 5′-CAGCTCATGACCCAGATAAGTGG-3′, reverse 5′-GTCTGCACAAGTGTACCATGTTGCG-3′ (787 bp); *PDE4C*: forward 5′-ATGGCCCAGATCACTGGGCTGCGG-3′, reverse 5′-GCTGAGGTTCTGGAAGATGTCGCAG-3′ (582 bp); *PDE4D*: forward 5′-CCCTCTTGACTGTTATCATGCACACC-3′, reverse 5′-GATCCTACATCATGTATTGCACTGGC-3′ (262 bp); *PDE5A*: forward 5′-CCCTGGCCTATTCAACAACGG-3′, reverse 5′-ACGTGGGTCAGGGCCTCATA-3′ (192 bp); *PDE7A*: forward 5′-GAAGAGGTTCCCACCCGTA-3′, reverse 5′-CTGATGTTTCTGGCGGAGA-3′ (85 bp); *PDE7B*: forward 5′-GGCTCCTTGCTCATTTGC-3′, 5′-GGAACTCATTCTGTCTGTTGATG-3′ (99 bp); PDE8A: forward 5′-TGGCAGCAATAAGGTTGAGA-3′, reverse 5′-CGAATGTTTCCTCCTGTCTTT-3′ (97 bp); *PDE8B*: forward 5′-CTCGGTCCTTCCTCTTCTCC-3′, 5′-AACTTCCCCGTGTTCTATTTGA-3′ (147 bp); *PDE9A*: forward 5′-GTGGGTGGACTGTTTACTGGA-3′, reverse 5′-TCGCTTTGGTCACTTTGTCTC-3′ (107 bp); *PDE10A*: forward 5′-

GACTTGATTGGCATCCTTGAA-3′, reverse 5′-CCTGGTGTATTGCTACGGAAG-3′ (115 bp); and *PDE11A*: forward 5′-CCCAGGCGATAAATAAGGTTC-3′, reverse 5′-TGCCACAGAATGGAAGATACA-3′ (87 bp).

All PCR products were run on a 2% agarose gel. The gel was visualised in the presence of ethidium bromide and imaged using a G Box iChemi gel documentation system. Density of each band was analysed with GeneTools analysis software (Syngene, UK). Correct band size was compared to that of previous works.

2.4 cAMP accumulation assay

Cells were grown to confluency in complete MEM growth medium. Cells were then trypsinised for 1 minute, re-suspended in stimulation buffer (PBS with 0.1% BSA) and plated onto 384-well optiplates (Perkin Elmer, UK) at a density of 2000 cells/well. To determine the efficacy of individual PDE inhibitors, cells were co-stimulated, immediately after seeding, with three different concentrations of compounds (which spanned 100-fold either side of the individual IC_{50} value in vitro) and pEC_{20} values of forskolin (1.6 μM for C6 cells and 50 nM for ST14A cells) for 30 minutes. Stimulating cells with the pEC_{20} of forskolin, enables a larger range to observe any effect of the PDE inhibitors on cAMP production. To generate full dose response curves, compounds were added to cells in the range of 0.1 pM – 100 μM for 30 minutes. Detection of cAMP was assessed using LANCE cAMP detection kit (Perkin Elmer, UK) and end-point measurement was performed using a Mithras LB940 microplate reader (Berthold Technologies, Germany). The lysed cells were excited at 340 nm wavelength with fluorescence from homogeneous time-resolved FRET detected at 665 nm.

To determine the effects of G proteins on cAMP production, C6 cells were grown in complete MEM medium in the presence of either PTX or CTX for 16 hours (as a pre-treatment). Subsequently, cells were dissociated using trypsin for 1 minute after which, complete medium was added to inactivate trypsin. Cells were washed, resuspended in PBS containing 0.1% BSA, and plated onto 384-well optiplates at a density of 8000 cells/well. Total accumulation of cAMP was determined using the same protocol as described above. Data were either normalised to the maximal level of cAMP accumulation from cells in response to 100 μM forskolin stimulation or were interpolated to the cAMP standard curve and expressed as the concentration cAMP per 10^6 cells. Where stated, cAMP levels are quoted as pmoles per mg of protein mass, determined using Bradford protein assay (Biorad, UK) following the manufacturer's instruction.

2.5 Determination of intracellular and extracellular cAMP levels

C6 cells were trypsinised and resuspended in PBS containing 0.1% BSA. 150,000 cells were then treated with various concentrations of PU23 (10 μM, 3.16 μM, and 1 μM, diluted in PBS containing 0.1% BSA) for 30 minutes. After treatment, cells were washed with PBS containing 0.1% BSA and stimulated with the pEC_{50} concentration of forskolin (3.16 μM), trequinsin (4.7 μM) or the PDE inhibitor cocktail (26 μM) for 1 or 2 hours, in the presence or absence of each concentration of PU23. After stimulation, cells were centrifuged at 1677 x g for 4 minutes to separate supernatant and cell pellet. LANCE cAMP detection kit (Perkin Elmer, UK) was used to determine extracellular cAMP levels (supernatant) and intracellular cAMP levels (cell pellet). The concentration of cAMP was determined by interpolating the HTR-FRET values to the cAMP standard curve. cAMP levels are expressed as the concentration per 10^6 cells.

2.6 cGMP accumulation assay

Confluent C6 cells were trypsinised and resuspended in PBS containing 0.1% BSA. Cells were plated onto a 384-well plate at a density of 500,000 cells/well and immediately stimulated with compounds for 30 minutes. After stimulation, 5 µl of d2-cGMP analogue and 5 µl mAb-cryptate were added to each well and incubated for 1 hour at room temperature as per the manufacturer's instruction (Cisbio, France). The d2-cGMP fluorophore was excited at a wavelength of 337 nm and emission was detected at 665 nm and 620 nm. Fluorescence was measured using a Mithras LB940 microplate reader (Berthold Technologies, Germany). Delta F% values were calculated using the 665 nm/620 nm ratio and all data were interpolated to a standard curve which covered an average cGMP range of 0.5 – 50 nM.

2.7 Cell proliferation assay

C6 cells were seeded at a density of 2,500 cells/well in a clear flat bottom 96-well plate (Corning). After 24 hours, cells were exposed to test compounds or vehicle, in complete MEM growth medium, and were incubated for 72 hours. To further investigate whether downstream pathways of cAMP influenced cell proliferation, cells were cotreated with selective inhibitors that target cAMP/cGMP sensors including PKA, PKG, and Epac. Cells were seeded as previously described and treated with either forskolin or trequinsin in the presence of the following inhibitors: KT5720 to inhibit PKA, KT5823 to inhibit PKG, ESI-09 as non-selective Epac inhibitor, CE3F4 as a selective Epac1 inhibitor, and HJC0350 as a selective Epac2 inhibitor. In order to investigate the effect of blockade of cAMP export on cell proliferation, cells were treated with forskolin, trequinsin or PDE inhibitor cocktail in the presence, or absence, of various concentrations of PU23 (10 µM, 3.16 µM, and 1 µM). After 72 hours

incubation, 5 μL of Cell Counting Kit – 8 (CCK-8, Sigma, UK) was added to each well and the cells were incubated for an additional 2-3 hours at 37 °C in the dark. The absorbance of each well was measured using a Mithras LB940 microplate reader (Berthold Technologies, Germany) with an excitation of 450 nm. The amount of formazan formed is directly proportional to the number of viable cells. Cell proliferation was calculated as a percentage of number of cells treated with vehicle alone.

2.8 Caspase assay

C6 cells were seeded into clear bottom black 96-well plates (Corning) and treated with forskolin (1-100 μM), trequinsin (1-100 μM) or staurosporine (1 μM, a pan caspase activator) in complete MEM media. 1% DMSO was used as vehicle control. Cells were exposed to test compounds for 72 hours, plates were treated with 2 μM of the CellEvent™Caspase-3/7 green detection reagent (Life Technologies, UK) for 60 minutes at 37 °C in the dark. Caspase activity was detected by cleavage of the tetrapeptide substrate DEVD, which is conjugated to a nucleic acid binding dye. Intracellular caspase-3/7 activities were imaged using a BD Pathway 855. To normalise the number of cells with caspase activated, cells were also labelled with Hoechst 33342 (Cambridge Bioscience, UK). Activated caspase-3/7 cleaves substrate and produce green fluorescence which was visualised using FITC/Alexa Fluor™ 488 filter setting. The total number of cells stained with Hoechst 33342 was measured using Hoechst filter (350/461 nm).

2.9 Cell Cycle Analysis

Cell cycle analysis using flow cytometry provides information on the distribution of cells in interphase stages of the cell cycle (G_0/G_1, S, and G_2/M). C6 cells were seeded in to

24-well plates and cultured for 24 hours. Cells were exposed to selected treatments including forskolin, trequinsin, and a combination of individual PDE2,3,7 inhibitor, for 72 hours. Subsequently, cells were harvested and resuspended in PBS containing 0.1% Triton X-100, 10 μg/ml RNase A, and 5 μg/ml propidium iodide (PI) before incubation at 37 °C for 15 minutes. Samples were analysed using a BD Accuri C6 flow cytometer and cell cycle analysis was performed using BD C6 software.

2.10 Statistical analysis

To quantify gene expression through RT-PCR, the densitometry results of each gene of interest were normalised to GAPDH signal. For cAMP accumulation and cell proliferation assays, data were fitted to obtain concentration–response curves using the three-parameter logistic equation using GraphPad Prism 8 (GraphPad Software, San Diego) to obtain values of E_{max} /I_{max}, pEC_{50}/pIC_{50}, baseline, and span. Statistical differences were analysed using one-way ANOVA followed by Dunnett's post-hoc (for comparisons amongst more than two groups) or independent Student's t-test (for comparison between two groups). To determine the correlation of cAMP levels and cell proliferation of each PDE inhibitor in both C6 and ST14A cells, Pearson's correlation coefficient (r) was calculated with 95% confidence interval. To compare the ability of compounds to suppress C6 cell proliferation a selection criterion was applied, whereby the term for affinity (pIC_{50}) was multiplied by the term for efficacy (span). Error for this composite measure was propagated by applying the following equation.

$$Pooled\ SEM = \sqrt{\left(\frac{SEM_A}{\bar{x}_A}\right)^2 + \left(\frac{SEM_B}{\bar{x}_B}\right)^2} \times \bar{x}_{AB}$$

Where, SEM_A and SEM_B are the standard errors of the mean of measurement A and B with mean of $\overline{x}_A$ and $\overline{x}_B$, $\overline{x}_{AB}$ is the composite mean.

3. RESULTS

3.1 Elevation of cAMP levels reduces cell proliferation in a glioma cell line

We first sought to determine if changes in cAMP concentration modulated glioma cell growth. When C6 cells, a rat-derived model for glioma, were exposed to the pan-AC activator, forskolin, we observed a dose-dependent increase in cAMP levels, up to 34,566 ± 9,346 nM per 10^6 cells which equates to 484.23 ± 134.11 pmol cAMP/mg protein (lysed cells) (Fig. 1A, 1B), and reduced cell proliferation (Fig. 1D).

Given the fact that there is crosstalk between the cAMP and cGMP pathways [30], we also evaluated the role of the cGMP pathway on cell proliferation by treating cells with the small molecule guanylyl cyclase activators, BAY 41-8543 and YC-1. Both compounds elevated cGMP levels (Fig. 1C), however, cGMP production was ~1000x lower than cAMP production in C6 cells, even in response to treatment with the nitric oxide (NO) donor, S-Nitroso-N-acetyl-DL-penicillamine (SNAP) (0.37 ± 0.04 pmol cGMP/mg protein). Surprisingly, both BAY 41-8543 and YC-1 also dose-dependently increased cAMP levels (Fig. 1A) but only ~20% relative to that of forskolin (Fig. 1A). BAY 41-8543 and YC-1 also had a minimal effect on cell proliferation compared to forskolin, with a reduction in cell survival only observed at 100 μM (Fig. 1D). These anti-proliferative effects may occur due to a modulatory effect between cAMP and cGMP. Accumulation of cGMP levels may lead to allosteric regulation of dual-substrate PDEs leading to potentiation of cAMP and suppression of cell growth. These results suggest that that elevation cAMP pathway plays a more important role in reducing cell proliferation.

Heterotrimeric G proteins are the primary effectors of G protein-coupled receptors (GPCRs) with $G\alpha_s$ activating AC and $G\alpha_{i/o}$ inhibiting AC [29]. Pertussis toxin (PTX) and cholera toxin (CTX) were utilised to determine whether G protein-mediated

cAMP production inhibits C6 cell growth. Treatment with CTX or PTX induced only a small elevation in cAMP levels and only suppressed C6 cell growth by 20% in a dose-dependent manner (Fig. 1D). Furthermore, despite potent stimulation of cAMP accumulation upon treatment with the non-selective β-adrenoceptor agonist, isoprenaline, suppression of cell growth was significantly poorer than treatment with forskolin. This implies that GPCR-mediated cAMP accumulation is insufficient to maximally supress C6 cell growth and is likely a result of transient effector activation, receptor desensitisation or spatially localised signalling. Together, these results suggest that increasing cAMP concentration, through direct pharmacological activation of AC, plays a pivotal role in inhibiting cell growth with a minimal involvement of cGMP.

3.2 Specific inhibition of PDEs indicates reliance on PDE expression levels

Given that intracellular concentrations of cAMP are modulated both by its production and degradation, we next sought to investigate the expression of PDEs in a glioma cell line. Reverse transcription PCR (rt-PCR) was performed to determine the expression of each PDE isoenzyme in C6 cells, compared to ST14A cells, a rodent model for healthy neurons. As shown in Fig. 2, the overall expression level of PDEs was higher in C6 cells compared to ST14A cells. With the exception of PDE1C, there was little overall difference in the profiles of PDEs expressed between C6 cells and ST14A cells. PDE1C, PDE4D, PDE7A, and PDE7B were the only PDEs to display significant elevation in C6 cells.

The rt-PCR expression profiles showed a wide number of PDEs to be expressed in glioma cells. However, this was only semi-quantitative, thereby, not providing a clear indication as to which PDEs might be the most important. Thus, we next investigated the role of PDEs in regulating cAMP levels and cell proliferation in

C6 cells by applying small molecule selective PDE inhibitors as tools to modify their action. The small compounds were blindly screened and subsequently decoded after data analysis (see methods). Both cell lines were stimulated with the pEC_{20} concentration of forskolin to increase the range for detecting an elevation of cAMP in the presence of selected PDE inhibitor. pEC_{50} values for cAMP production and pIC_{50} values for cell growth inhibition for each compound are quoted in Table 1 and their pharmacological actions are summarised in Table 2.

Plotting the potencies of each PDE inhibitor revealed a significant ($p<0.001$) positive correlation between elevation of cAMP levels and inhibition of cell growth (Fig. 3A and 3B) for both C6 cells ($r = 0.83$ (95% confidence interval 0.46–0.95)) and ST14A cells ($r = 0.97$ (95% confidence interval (0.73–0.99)). To provide a convenient and rapid method for comparing each PDE inhibitor for effects on cell growth, the terms for efficacy and affinity (potency and span values) were multiplied for both C6 and ST14A cells (arbitrary units – Fig. 3C and 3D). An ideal compound would be one that shows high potency for inhibition of growth and a large range. An arbitrary threshold of 200 was set to determine compounds that might be worth further investigation. Cisplatin, a widely used non-selective anti-proliferative agent, was used as a reference to validate our method (with pIC_{50} of 6.02 and 5.92 in C6 and ST14A cells, respectively, Table 1). In both C6 and ST14A cells, cisplatin showed the highest selection criteria value (582.1 in C6 cells and 511.1 in ST14A cells), thus proving that this calculation may help to determine how effective the compounds are at inhibiting cell proliferation. From our initial screen only 9 compounds were deemed to have passed the threshold: vinpocetine (PDE1 inhibitor), amrinone, milrinone (both PDE3 inhibitors), ibudilast (PDE4 inhibitor), trequinsin, IBMX and zaprinast (multiple PDE isoform inhibitors), BRL50481 (PDE7 inhibitor), and forskolin. The selectivity of the inhibitors that were

successful in the screen correlated well with PDE expression levels in C6 cells (Fig. 2A and 2B). The compounds that showed the highest values (>350) were forskolin, trequinsin, amrinone, and IBMX. Apart from amrinone, these compounds target multiple components in the cAMP synthesis/degradation pathway, thus explaining their greater affinity/efficacy. IBMX and zaprinast were not used in future studies due to selectivity issues. IBMX is an adenosine receptor antagonist [31], whilst zaprinast is a GPR35 agonist [32]. Finally, it is worth noting that all compounds displayed lower affinity/efficacy values in ST14A cells (Fig. 3D) and this is consistent with the reduced PDE expression compared to C6 cells (Fig. 2B).

3.3 Cocktail of individual PDE2, PDE3, and PDE7 inhibitors exhibited a similar effect to that of trequinsin, both upon elevating cAMP levels and suppressing cell growth

Of all the compounds tested, trequinsin was the most potent at increasing cAMP levels and suppressing cell growth. Trequinsin is known to potently inhibit PDE3, but is suggested to also block the cAMP binding site of PDE2 and PDE7 [26]. This, however, has not been thoroughly investigated. Therefore, we probed the mechanism by which trequinsin exerts its antiproliferative effects by combining selective inhibitors against PDE2, PDE3, and PDE7 – by using EHNA, amrinone, and BRL-50481, respectively.

None of the selective PDE inhibitors were more potent at stimulating cAMP accumulation or inhibiting cell proliferation in C6 cells, as individual treatments, than trequinsin (Fig. 4A and 4D). Although amrinone displayed a similar E_{max} to that of trequinsin for cAMP accumulation, the I_{max} for cell growth inhibition was ~50% relative to trequinsin (Fig. 4A and 4D, Table 3). Subsequently, we investigated the combinatorial effect of individual PDE2, 3, and 7 inhibitors. The combination of EHNA

and amrinone (PDE2 and PDE3 inhibitors), as well as EHNA and BRL-50481 (PDE2 and PDE7 inhibitors), enhanced the potency of effect compared to when these drugs were used individually (Fig. 4B and 4E, Table 3). However, the combination of BRL-50481 with amrinone (PDE3 and PDE7 inhibitors) was comparable to that of amrinone alone. Interestingly, when all three selective inhibitors were combined, the potency and efficacy were similar to that of trequinsin (Fig. 4C and 4F, Table 3). Overall, this suggests that simultaneous inhibition of PDE2, PDE3, and PDE7 can mimic the antiproliferative effect of trequinsin.

3.4 Targeting both AC and PDEs enhances the anti-proliferative effect

Our data suggests that elevation of cAMP levels through either, activation of AC, or inhibition of PDEs, positively correlates with reduced cell proliferation. Thus, we hypothesised that dual activation of AC and inhibition of PDEs would induce larger suppression in cell growth beyond that of a single target treatment. To test this, we determined the combinatorial effect of forskolin and trequinsin on cAMP accumulation and cell proliferation (Fig. 5).

There was a similar pattern of effects observed upon forskolin and trequinsin co-treatment on both cAMP accumulation and cell proliferation assays. The combination of forskolin and trequinsin significantly enhanced cAMP accumulation and reduced C6 cell growth in a dose-dependent manner compared to forskolin alone (Fig. 5A-C). The potency of the forskolin-mediated anti-proliferative effect was enhanced approximately 10-fold in the presence of 10 μM trequinsin (pIC_{50} of forskolin is 5.75, that of forskolin in combination with 10 μM trequinsin is 6.87). These data demonstrate synergistic elevation of cAMP by targeting AC and PDEs resulting in greater suppression of C6 cell growth. Indeed, the effect of the combination of 1 μM

forskolin and 0.1 μM trequinsin was approximately equal to that of cisplatin (pIC_{50} of 6.09, Table 1).

3.5 Blockade of cAMP export enhances the anti-proliferative effect of forskolin, trequinsin, and the PDE inhibitor cocktail

C6 cells are known to express MRP4 [33] a transporter known to export intracellular cAMP. Having confirmed that inhibiting PDEs, or activating AC, elevates total cAMP levels and supresses proliferation of C6 cells, we aimed to investigate if these effects could be enhanced by preventing cellular export of cAMP.

Pre-treatment with PU23, a small molecule inhibitor of MRP4, resulted in a dose-dependent reduction in extracellular cAMP levels post stimulation with forskolin, trequinsin or the PDE inhibitor cocktail (Fig.6A, C and D). There was also a substantial elevation in intracellular concentrations of cAMP in the presence of PU23 after 2 hours stimulation with forskolin (Fig. 6B). This suggests that in the absence of PDE inhibitor, blockade of cAMP export maintains high intracellular cAMP levels. Indeed, the combination of PU23 with forskolin, trequinsin, or the PDE inhibitor cocktail enhanced the anti-proliferative effect of each compound (Fig.6 E-G). Taken together, these data suggest that suppression of C6 cell proliferation can be enhanced by blockade of cAMP export.

3.6 The anti-proliferative effect of forskolin is mediated through a PKA-dependent mechanism

Having confirmed the effect of cAMP on C6 cell growth, we next wanted to investigate the involvement of downstream effectors of cAMP, such as PKA and Epac type I and II, as well as the cGMP effector, PKG, and GC activation on proliferation of

C6 cells (Fig. 7A). To do this, we utilised a range of small molecule inhibitors: KT5720 (PKA), ESI-09 (non-selective Epac), CE3F4 (Epac1), HJC0350 (Epac2), and KT5823 (PKG), and the GC activator (BAY 41-8543). Co-treatment of 10 μM KT5720 significantly attenuated the anti-proliferative effects of forskolin ($p<0.01$), trequinsin ($p<0.001$) and the PDE inhibitor cocktail ($p<0.05$) on C6 cells (Fig. 7B-D). None of the selective or non-selective Epac inhibitors had any effect on trequinsin-mediated cell growth suppression, although there was an elevation of forskolin-mediated cell growth suppression with CE3F4 ($p<0.01$) (Fig. 7B). Interestingly, cotreatment with KT5823 significantly enhanced the anti-proliferative effects of forskolin and trequinsin ($p<0.001$), whilst BAY 41-8543 treatment also increased forskolin-mediated suppression of cell proliferation ($p<0.01$). This indicates an involvement of cGMP signalling pathways in cell proliferation. It is possible that accumulation of cGMP, in the presence of the PKG inhibitor or GC activator, potentiates cAMP/PKA signalling pathways through the sequestration of non-selective PDEs, thereby reducing cell growth. There was, however, no significant effect of BAY 41-8543 treatment on the anti-proliferative effects of trequinsin or the PDE inhibitor cocktail. This may suggest that the actions observed for KT5823 are not purely due to inhibition of PKG. These data highlight the importance of the homeostasis between cAMP and cGMP, as well as that the anti-proliferative effects of forskolin, trequinsin and the PDE inhibitor cocktail are largely mediated through a cAMP/PKA-dependent pathway.

3.7 Trequinsin, but not forskolin or the PDE inhibitor cocktail, has cAMP-independent actions leading to apoptosis

In order to delineate the mechanism by which cAMP promotes cell death or inhibits cell growth, we investigated if the anti-proliferative effects on C6 cells were related to

apoptosis. Early apoptotic events can be detected through the protease activity of caspase-3 and caspase-7 that will eventually degrade proteins pivotal for cell survival. In this study, we quantified cells positive for caspase-3 and -7 activity in C6 cells using fluorescence microscopy after treatment with CellEvent™ Caspase-3/-7 green detection kit. Cells were co-stained with Hoechst 33342 and propidium iodide to label all nuclei and dead cells.

Staurosporine is a known pan caspase activator. Quantitative analysis revealed that staurosporine-treated cells were entirely positive for active caspase-3/-7 (Fig. 8A). Consistent with these results, activated caspase-3/-7 resulted in cell death which was confirmed by propidium iodide staining (Fig. 8A). Among all other treatments, only 100 μM trequinsin exhibited comparable effects on cell death and caspase activity to that of staurosporine. Treatment with forskolin or the PDE 2,3,7 inhibitor cocktail resulted in less than 10% caspase activity and cell death (Fig. 7A). This suggests that 100 μM trequinsin may have toxic, non-cAMP-dependent effects, on C6 cells.

3.8 Elevated intracellular cAMP induces growth arrest at the G_2/M phase of the cell cycle

Having demonstrated that elevation of cAMP inhibits cell proliferation, without inducing extensive apoptotic events on cells treated with forskolin, PDE inhibitor cocktail, or a low concentration of trequinsin, we postulated that this effect arose due to cell growth arrest. Thus, we investigated the individual stages of the cell cycle of C6 cells post-treatment with forskolin, trequinsin or the PDE2,3,7 inhibitor cocktail by using propidium iodide staining and flow cytometry. Cell cycle analysis showed that forskolin, trequinsin, and the PDE2,3,7 inhibitor cocktail altered the cell phase (Fig. 8B-E). While there was no significant difference between complete media and DMSO,

forskolin or PDE inhibitor cocktail treated cells arrested predominantly in G_2/M phase. This indicates that both forskolin and the PDE2,3,7 inhibitor cocktail alter C6 cell cycle by a similar mechanism. In contrast, of the proportion of cells that survived treatment with 100 μM trequinsin, approximately 70% were aneuploid, with the remaining alive cells arrested in G_2/M phase. Interestingly, when lower concentrations of trequinsin (<100 μM) were considered, the cell phase profile more closely matched that of 10 μM PDE2,3,7 inhibitor cocktail (Fig. 8B). This data suggests that 100 μM trequinsin induces a toxic effect on the C6 cells that is most likely independent of its action upon the cAMP pathway.

4. DISCUSSION

cAMP is a ubiquitous second messenger, which together with cGMP, controls a myriad of physiological responses [34] including reparative processes. Interestingly, cAMP signalling has been reported to have different effects on cell proliferation; either causing or arresting proliferation, depending on the cell type investigated [9, 13, 35]. These divergent effects of cAMP on the proliferative response are believed to be controlled by several factors including stimulus, the nature of the intracellular cAMP effectors within the cells, the strength of signal, and subcellular compartmentalisation [36]. In brain tumours, suppression of cAMP is associated with gliomagenesis compared to non-tumour controls [37, 38]. As cAMP levels are suppressed 4-fold in brain tumours compared to those in normal tissue [5], we hypothesised that augmenting production of cAMP may restore intracellular signalling and have beneficial antiproliferative effects.

Although PDEs have long been targets for pharmacological modulation, there have been no studies characterising PDE isoenzyme expression in glioma cells or the

effect of PDE modulation. In the present study, we demonstrate that direct pharmacological activation of AC and inhibition of PDEs results in greater suppression of glioma cell proliferation than G protein-mediated AC activation. Although activation of G_s-coupled β-ARs by isoprenaline, or modulation of G protein activity by PTX or CTX treatment increased cAMP production, neither substantially suppressed glioma cell growth. This is possibly due to only transient activation of cAMP effectors, receptor desensitisation, spatially localised cAMP accumulation, or, the instability of isoprenaline in aqueous solution. Prolonged stimulation with GPCR agonists not only induces desensitisation through receptor internalisation, but may also alter transcription levels resulting in receptor downregulation [39]. It is worth noting that addition of antioxidant such as ascorbic acid or EDTA may be useful to minimise the degradation of isoprenaline during the treatment.

Evaluation of PDE mRNA expression level in C6 cells revealed that almost all PDE isoenzymes are expressed. Interestingly, inhibitors of cAMP-specific or cGMP-specific PDEs showed minimal effects on cell growth, except for ibudilast (a cAMP-specific PDE4 inhibitor). Inhibition of PDE1, PDE2, PDE3, PDE4, and PDE7 resulted in greater modulation of cAMP levels and cell growth. These PDEs, with the exception of PDE4 and PDE7, hydrolyse both cAMP and cGMP. Dual substrate PDEs provide a point for crosstalk between cGMP and cAMP signalling pathways and have unique mechanisms of regulation [40, 41].

The most potent anti-proliferative effects were observed in trequinsin-treated cells. Trequinsin is commonly known as an ultrapotent PDE3 inhibitor, although it has also been shown to have activity against PDE2 and PDE7 [26]. There have, however, been no studies into inhibition of PDE2 and PDE7 by trequinsin. A combination of inhibitors of PDE2, PDE3, and PDE7, the PDE inhibitor cocktail, had a similar

magnitude of effect to that of trequinsin, whilst inhibition of single or dual PDEs failed to mimic the effect. In order to enhance antiproliferative activity further, the selectivity of individual compounds towards each PDE needs to be improved.

Through the use of several pharmacological tools we attributed forskolin and trequinsin, and the PDE inhibitor cocktail mediated inhibition of cell growth to enhanced activation of PKA. Considering the greater affinity of cAMP for PKA than Epac1/2 (5-24.6 nM versus 4 μM/1.2 μM, respectively) [42-44], it is possible that elevated cAMP, upon treatment with forskolin or PDE inhibitors will preferentially activate PKA over Epac1/2. Taken together, there is a possibility that stimulation of AC by forskolin or by PDE inhibitors will trigger massive production of cAMP and consequently the PKA pathway will be predominantly activated with minor involvement of Epac1/2. The inhibitory action of cAMP on cell growth has also been reported to involve a complex mechanism between PKA, MAPK/ERK, and cyclin-dependent kinase 2 [45, 46].

Somewhat unexpectedly, this study demonstrated that PKG inhibition increased the anti-proliferative effects of forskolin- and trequinsin- treated cells, whilst GC activation also potentiated forskolin-mediated cell growth suppression. This is most likely due to cross talk between the cGMP and cAMP pathways via dual substrate PDEs. For instance, while cGMP binding to PDE2 allosterically enhances hydrolysis of cAMP, cGMP competitively inhibits PDE3 to reduce the rate of cAMP breakdown . This control is, however, dependent on the concentration of cGMP, with allosteric regulation of PDE2 requiring higher (1-5 μM) [47] cGMP levels than the affinity of cGMP for the catalytic site of PDE3 (180 nM) [17]. We have shown that C6 cells have a weaker propensity to elevate cGMP levels than cAMP. Thus, a modest increase in cGMP may compete with cAMP to occupy catalytic sites resulting in a decrease in the

hydrolysis rate of cAMP by dual substrate PDE isoforms, thus activating the cAMP/PKA pathway triggering enhanced cell growth suppression.

Surprisingly, there was no effect of PKG inhibition or GC activation on the anti-proliferative effects of the PDE inhibitor cocktail. Whilst this may suggest that the actions observed for KT5823 are not purely due to inhibition of PKG the functional effect of the PDE inhibitor cocktail may be affected by compartmentalisation and local activation of PKA. A small increase in cGMP may elevate cAMP levels only in distinct subcellular regions in the presence of the PDE inhibitor cocktail to activate PKA through anchoring proteins (AKAP) to different intracellular microstructures [47]. Although further investigation is required, these phenomena can be taken into account in explaining the differential responses observed upon PDE inhibitor cocktail treatment.

Although trequinsin has a comparable potency to that of forskolin for elevating intracellular cAMP levels and supressing cell proliferation, at high concentrations (100 μM) trequinsin induced substantial cell death of C6 cells and ST14A cells. This implies that at such high concentrations trequinsin binds to other non-PDE proteins that results in direct activation of caspase-3/7 to trigger cell death. Adequate activation of PKA will activate p53 and induce apoptosis [48] although we observed only less than 10% cell death. Nonetheless, the remaining cells were aneuploidy with at least 4N. It is likely that cells underwent faulty cell division and were not able to exit the mitotic state due to rapid and massive elevation of cAMP by 100 μM trequinsin. There are no studies on the mechanism by which trequinsin causes aneuploidy and apoptosis, however, there are several reports that in other types of cancer where cAMP levels are elevated by PDE inhibition, activation of PKA resulted in activation of protein phosphatase 2A

(PP2A) and Bim/BAD expression [13] that eventually cleaves caspases to mediate apoptosis.

Despite this, the study demonstrates that multitarget enhancement of cAMP signalling elevates anti-proliferative effects in a glioma cell model. Increasing cAMP levels through activation of AC (forskolin) and multiple PDE inhibition (by trequinsin) demonstrated synergistic cell growth suppression. Similarly, whilst it has been suggested that cyclic nucleotide efflux pumps may not contribute to controlling cAMP signalling [49], our study shows that inhibiting export of cAMP significantly enhances forskolin and multiple PDE inhibition mediated cell growth suppression. Thus, the dose of each compound could be reduced to potentially prevent any toxic side effects from trequinsin. Alternatively, combining individual selective inhibitors against PDE2,3,7 together showed similar efficacy to that of trequinsin but without significant toxicity in glioma cells. The inhibitor cocktail shows a higher number of cells with active caspase-3/7 activity compared to forskolin, possibly due to the availability of PDEs, which have been shown to be caspase substrates [13]. Both forskolin and the inhibitor cocktail trapped cells in G_2/M phase, which may lead to the loss of essential cellular components that are required for replication. Whilst this study has demonstrated that targeting the cyclic nucleotide pathway can suppress C6 cell growth, it should be noted that PDEs play an important role in many systems throughout the body, including the cardiovascular system, and thus targeting PDEs may cause off-target effects.

In conclusion, we have used a chemical biology approach to demonstrate that cAMP inhibits growth of glioma cells. Anti-proliferative effects of forskolin are mediated by elevating cAMP levels leading to activation of PKA and arrest of cells in the G_2/M phase of the cell cycle. In comparison, multiple inhibition of PDEs by trequinsin not only inhibits cell growth via the cAMP/PKA cascade, but also triggers cell death

through caspase-3/-7 activation. Concomitant targeting of both AC and PDEs synergistically elevates intracellular cAMP levels within glioma cells. Due to possible side effects of trequinsin, a cocktail of individual PDE2, PDE3, and PDE7 inhibitors can be used as an alternative to trequinsin to obtain similar functional effects without any toxicity. This study offers insight to identify new therapeutic approaches which have potential beneficial effects against glioma/glioblastoma.

AUTHOR CONTRIBUTIONS

DS, MH, LK, FS, DB, GL conceived and designed the research; DS, HP, HYY, IW performed the experiments; DS, MTH, TR, and GL analyzed data; DS, MH, HYY and GL wrote manuscript, DB, LK, TR, MTH revised and edited the manuscript.

ACKNOWLEDGEMENTS

Authors acknowledge the support of Endowment Fund for education from Ministry of Finance Republic of Indonesia (DS), a BBSRC Flexible Talent Mobility Account scheme award (GL and LK), BBSRC Doctoral Training Partnership BB/JO1454/1 (MH), Rosetrees Trust (to HYY and GL), and the Brain Tumour Charity (UK) grant GN-000429 (LK, FS, DB). HYY is also supported by the Cambridge Trust International Scholarship. We thank Sampurna Chakrabarty for support throughout preparation of this article. Finally, we would like to thank Colin Taylor for the C6 cell line.

DECLARATIONS

DB and LK are current employees of *IOTA Pharmaceuticals Ltd*; FS is a former employee.

REFERENCES

[1] A.N. Mamelak, D.B. Jacoby, Targeted delivery of antitumoral therapy to glioma and other malignancies with synthetic chlorotoxin (TM-601), Expert Opin Drug Deliv 4(2) (2007) 175-86.

[2] M. Harris, F. Svensson, L. Kopanitsa, G. Ladds, D. Bailey, Emerging patents in the therapeutic areas of glioma and glioblastoma, Expert Opin Ther Pat 28(7) (2018) 573-590.

[3] J.A. Schwartzbaum, J.L. Fisher, K.D. Aldape, M. Wrensch, Epidemiology and molecular pathology of glioma, Nat Clin Pract Neurol 2(9) (2006) 494-503; quiz 1 p following 516.

[4] H. Mao, D.G. Lebrun, J. Yang, V.F. Zhu, M. Li, Deregulated signaling pathways in glioblastoma multiforme: molecular mechanisms and therapeutic targets, Cancer Invest 30(1) (2012) 48-56.

[5] M.A. Furman, K. Shulman, Cyclic AMP and adenyl cyclase in brain tumors, J Neurosurg 46(4) (1977) 477-83.

[6] M. Illiano, L. Sapio, A. Salzillo, L. Capasso, I. Caiafa, E. Chiosi, A. Spina, S. Naviglio, Forskolin improves sensitivity to doxorubicin of triple negative breast cancer cells via Protein Kinase A-mediated ERK1/2 inhibition, Biochemical Pharmacology 152 (2018) 104-113.

[7] L. Hirsh, A. Dantes, B.S. Suh, Y. Yoshida, K. Hosokawa, K. Tajima, F. Kotsuji, O. Merimsky, A. Amsterdam, Phosphodiesterase inhibitors as anti-cancer drugs, Biochemical Pharmacology 68(6) (2004) 981-988.

[8] T.W. Kang, S.W. Choi, S.R. Yang, T.H. Shin, H.S. Kim, K.R. Yu, I.S. Hong, S. Ro, J.M. Cho, K.S. Kang, Growth arrest and forced differentiation of human primary glioblastoma multiforme by a novel small molecule, Sci Rep-Uk 4 (2014).

[9] A. Sawa, T. Chiba, J. Ishii, H. Yamamoto, H. Hara, H. Kamma, Effects of sorafenib and an adenylyl cyclase activator on in vitro growth of well-differentiated thyroid cancer cells, Endocr J (2017).

[10] I.H. Zwain, P. Amato, cAMP-induced apoptosis in granulosa cells is associated with up-regulation of P53 and bax and down-regulation of clusterin, Endocr Res 27(1-2) (2001) 233-249.

[11] E. Huston, T.M. Houslay, G.S. Baillie, M.D. Houslay, cAMP phosphodiesterase-4A1 (PDE4A1) has provided the paradigm for the intracellular targeting of phosphodiesterases, a process that underpins compartmentalized cAMP signalling, Biochem Soc Trans 34(Pt 4) (2006) 504-9.

[12] B. Ding, J.I. Abe, H. Wei, Q.H. Huang, R.A. Walsh, C.A. Molina, A. Zhao, J. Sadoshima, B.C. Blaxall, B.C. Berk, C. Yan, Functional role of phosphodiesterase 3 in cardiomyocyte apoptosis - Implication in heart failure, Circulation 111(19) (2005) 2469-2476.

[13] A. Lerner, P.M. Epstein, Cyclic nucleotide phosphodiesterases as targets for treatment of haematological malignancies, Biochem J 393(Pt 1) (2006) 21-41.

[14] J.A. Beavo, Cyclic nucleotide phosphodiesterases: functional implications of multiple isoforms, Physiol Rev 75(4) (1995) 725-48.

[15] S.H. Soderling, J.A. Beavo, Regulation of cAMP and cGMP signaling: new phosphodiesterases and new functions, Curr Opin Cell Biol 12(2) (2000) 174-9.

[16] F.S. Menniti, W.S. Faraci, C.J. Schmidt, Phosphodiesterases in the CNS: targets for drug development, Nat Rev Drug Discov 5(8) (2006) 660-70.

[17] K. Omori, J. Kotera, Overview of PDEs and their regulation, Circ Res 100(3) (2007) 309-27.

[18] S.H. Francis, M.A. Blount, J.D. Corbin, Mammalian cyclic nucleotide phosphodiesterases: molecular mechanisms and physiological functions, Physiol Rev 91(2) (2011) 651-90.

[19] M. Conti, D. Mika, W. Richter, Cyclic AMP compartments and signaling specificity: role of cyclic nucleotide phosphodiesterases, J Gen Physiol 143(1) (2014) 29-38.

[20] Y. Ladilov, A. Appukuttan, Role of soluble adenylyl cyclase in cell death and growth, Biochim Biophys Acta 1842(12 Pt B) (2014) 2646-55.

[21] R. Sengupta, T. Sun, N.M. Warrington, J.B. Rubin, Treating brain tumors with PDE4 inhibitors, Trends in Pharmacological Sciences 32(6) (2011) 337-344.

[22] V. Cesarini, M. Martini, L.R. Vitiani, G.L. Gravina, S. Di Agostino, G. Graziani, Q.G. D'Alessandris, R. Pallini, L.M. Larocca, P. Rossi, E.A. Jannini, S. Dolci, Type 5 phosphodiesterase regulates glioblastoma multiforme aggressiveness and clinical outcome, Oncotarget 8(8) (2017) 13223-13239.

[23] R. Savai, S.S. Pullamsetti, G.A. Banat, N. Weissmann, H.A. Ghofrani, F. Grimminger, R.T. Schermuly, Targeting cancer with phosphodiesterase inhibitors, Expert Opin Inv Drug 19(1) (2010) 117-131.

[24] M.D. Brooks, E. Jackson, N.M. Warrington, J. Luo, J.T. Forys, S. Taylor, D.D. Mao, J.R. Leonard, A.H. Kim, D. Piwnica-Worms, R.D. Mitra, J.B. Rubin, PDE7B Is a Novel, Prognostically Significant Mediator of Glioblastoma Growth Whose Expression Is Regulated by Endothelial Cells, PLOS ONE 9(9) (2014) e107397.

[25] R.W. Chen, A.J. Williams, Z.L. Liao, C.P. Yao, F.C. Tortella, J.R. Dave, Broad spectrum neuroprotection profile of phosphodiesterase inhibitors as related to

modulation of cell-cycle elements and caspase-3 activation, Neuroscience Letters 418(2) (2007) 165-169.

[26] R.J. Rickles, L.T. Pierce, T.P. Giordano, W.F. Tam, D.W. McMillin, J. Delmore, J.P. Laubach, A.A. Borisy, P.G. Richardson, M.S. Lee, Adenosine A2A receptor agonists and PDE inhibitors: a synergistic multitarget mechanism discovered through systematic combination screening in B-cell malignancies, Blood 116(4) (2010) 593-602.

[27] M.E. Ehrlich, L. Conti, M. Toselli, L. Taglietti, E. Fiorillo, V. Taglietti, S. Ivkovic, B. Guinea, A. Tranberg, S. Sipione, D. Rigamonti, E. Cattaneo, ST14A cells have properties of a medium-size spiny neuron, Experimental Neurology 167(2) (2001) 215-226.

[28] A.G. Gilman, Regulation of adenylyl cyclase by G proteins, Adv Second Messenger Phosphoprotein Res 24 (1990) 51-7.

[29] J.D. Hildebrandt, Role of subunit diversity in signaling by heterotrimeric G proteins, Biochem Pharmacol 54(3) (1997) 325-39.

[30] M. Zaccolo, M.A. Movsesian, cAMP and cGMP signaling cross-talk: role of phosphodiesterases and implications for cardiac pathophysiology, Circ Res 100(11) (2007) 1569-78.

[31] A.J. Morgan, K.J. Murray, R.A. Challiss, Comparison of the effect of isobutylmethylxanthine and phosphodiesterase-selective inhibitors on cAMP levels in SH-SY5Y neuroblastoma cells, Biochem Pharmacol 45(12) (1993) 2373-80.

[32] Y. Taniguchi, H. Tonai-Kachi, K. Shinjo, Zaprinast, a well-known cyclic guanosine monophosphate-specific phosphodiesterase inhibitor, is an agonist for GPR35, FEBS Lett 580(21) (2006) 5003-8.

[33] X. Decleves, S. Bihorel, M. Debray, S. Yousif, G. Camenisch, J.M. Scherrmann, ABC transporters and the accumulation of imatinib and its active metabolite CGP74588 in rat C6 glioma cells, Pharmacol Res 57(3) (2008) 214-22.

[34] E.W. Sutherland, Studies on the mechanism of hormone action, Science 177(4047) (1972) 401-8.

[35] K.A. Cullen, J. McCool, M.S. Anwer, C.R.L. Webster, Activation of cAMP-guanine exchange factor confers PKA-independent protection from hepatocyte apoptosis, Am J Physiol-Gastr L 287(2) (2004) G334-G343.

[36] P.A. Insel, L. Zhang, F. Murray, H. Yokouchi, A.C. Zambon, Cyclic AMP is both a pro-apoptotic and anti-apoptotic second messenger, Acta Physiol 204(2) (2012) 277-287.

[37] N.M. Warrington, S.M. Gianino, E. Jackson, P. Goldhoff, J.R. Garbow, D. Piwnica-Worms, D.H. Gutmann, J.B. Rubin, Cyclic AMP Suppression Is Sufficient to Induce Gliomagenesis in a Mouse Model of Neurofibromatosis-1, Cancer Research 70(14) (2010) 5717-5727.

[38] P.M. Daniel, G. Filiz, T. Mantamadiotis, Sensitivity of GBM cells to cAMP agonist-mediated apoptosis correlates with CD44 expression and agonist resistance with MAPK signaling, Cell Death & Disease 7 (2016).

[39] W.P. Hausdorff, M.G. Caron, R.J. Lefkowitz, Turning off the signal: desensitization of beta-adrenergic receptor function, FASEB J 4(11) (1990) 2881-9.

[40] J. Surapisitchat, K.I. Jeon, C. Yan, J.A. Beavo, Differential regulation of endothelial cell permeability by cGMP via phosphodiesterases 2 and 3, Circ Res 101(8) (2007) 811-8.

[41] S.H. Francis, J.L. Busch, J.D. Corbin, D. Sibley, cGMP-dependent protein kinases and cGMP phosphodiesterases in nitric oxide and cGMP action, Pharmacol Rev 62(3) (2010) 525-63.

[42] J. de Rooij, F.J.T. Zwartkruis, M.H.G. Verheijen, R.H. Cool, S.M.B. Nijman, A. Wittinghofer, J.L. Bos, Epac is a Rap1 guanine-nucleotide-exchange factor directly activated by cyclic AMP, Nature 396(6710) (1998) 474-477.

[43] J. Bubis, L.D. Saraswat, S.S. Taylor, Tyrosine-371 contributes to the positive cooperativity between the two cAMP binding sites in the regulatory subunit of cAMP-dependent protein kinase I, Biochemistry 27(5) (1988) 1570-1576.

[44] G.E. Ringheim, S.S. Taylor, Effects of cAMP-binding site mutations on intradomain cross-communication in the regulatory subunit of cAMP-dependent protein kinase I, J Biol Chem 265(32) (1990) 19472-8.

[45] L. Favot, T. Keravis, V. Holl, A. Le Bec, C. Lugnier, VEGF-induced HUVEC migration and proliferation are decreased by PDE2 and PDE4 inhibitors, Thromb Haemost 90(2) (2003) 334-43.

[46] P.K. Vadiveloo, E.L. Filonzi, H.R. Stanton, J.A. Hamilton, G1 phase arrest of human smooth muscle cells by heparin, IL-4 and cAMP is linked to repression of cyclin D1 and cdk2, Atherosclerosis 133(1) (1997) 61-9.

[47] T. Keravis, C. Lugnier, Cyclic nucleotide phosphodiesterase (PDE) isozymes as targets of the intracellular signalling network: benefits of PDE inhibitors in various diseases and perspectives for future therapeutic developments, Brit J Pharmacol 165(5) (2012) 1288-1305.

[48] T. Fujita, Y. Ishikawa, Apoptosis in heart failure. -The role of the beta-adrenergic receptor-mediated signaling pathway and p53-mediated signaling pathway in the apoptosis of cardiomyocytes, Circ J 75(8) (2011) 1811-8.

[49] M. Adachi, G. Reid, J.D. Schuetz, Therapeutic and biological importance of getting nucleotides out of cells: a case for the ABC transporters, MRP4 and 5, Adv Drug Deliv Rev 54(10) (2002) 1333-42.

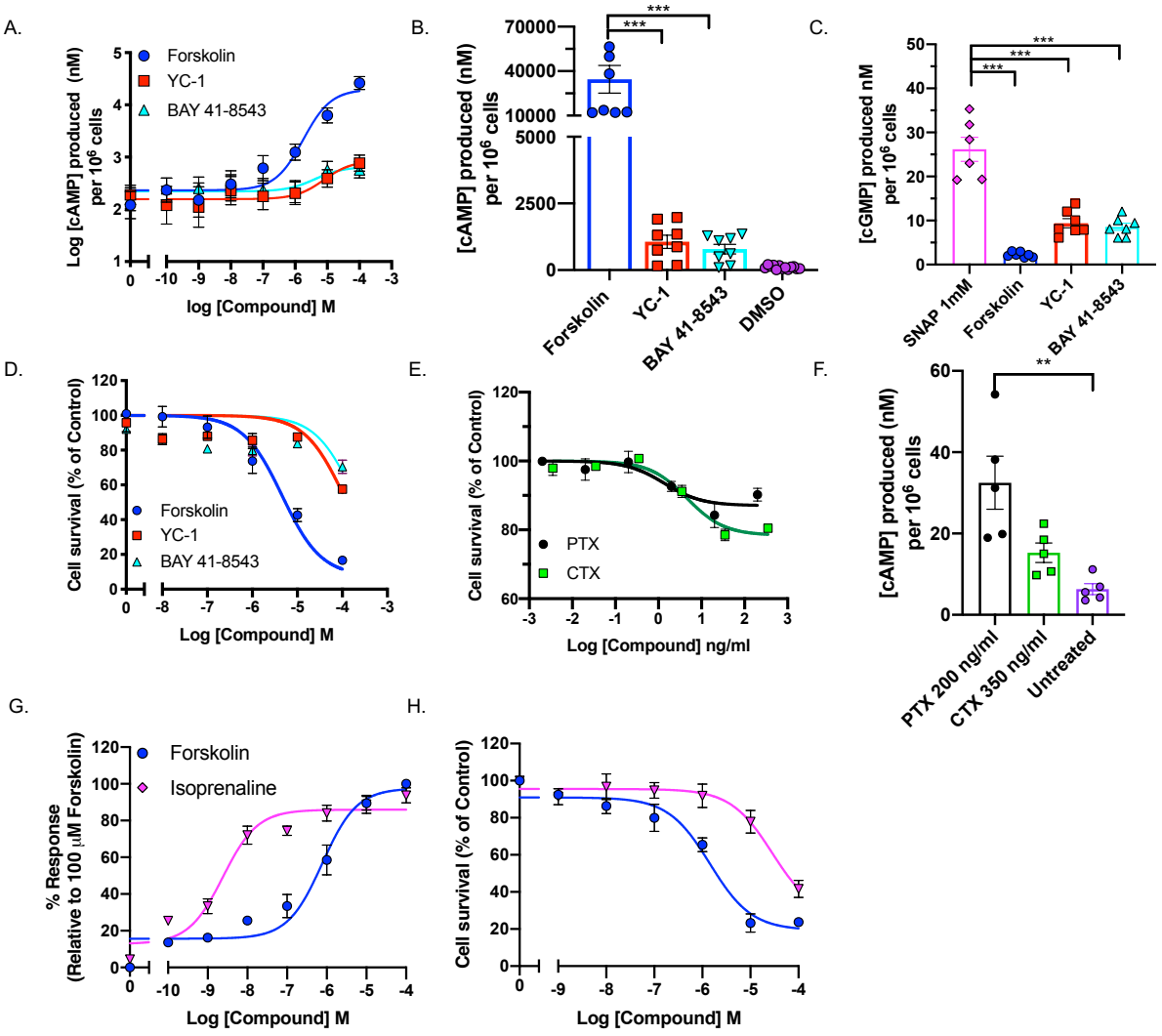

Fig. 1. Elevation of cAMP, but not cGMP, mediates cell growth suppression. *A*. cAMP levels following 30 minutes treatment with adenylyl cyclase activator (forskolin) or guanylyl cyclase activators (YC-1 and BAY 41-8543). *B-C*. Comparison of accumulation of cAMP and cGMP in C6 cells in response to forskolin (100 μM), BAY 41-8543 (100 μM), YC-1 (100 μM), or SNAP (100 μM). Survival of C6 cells following 72 hours treatment with forskolin, BAY 41-8543 or YC-1 (D) or PTX or CTX (E). *F*. cAMP levels after 16 hours pre-treatment with PTX or CTX in comparison to untreated cells. *G.* cAMP levels in C6 cells following 30 minutes stimulation with forskolin or the non-selective beta-adrenergic agonist,

isoprenaline. Data are expressed relative to 100 μM forskolin *H.* Cell survival of C6 cells following 72 hours treatment with forskolin or isoprenaline. Data are expressed as percentage survival relative to vehicle alone and are the mean±SEM of 6-9 individual experiments. Statistical significance was determined using a one-way analysis of variance followed by Dunnett's *post hoc* test (*, $p<0.05$; ***, $p<0.001$).

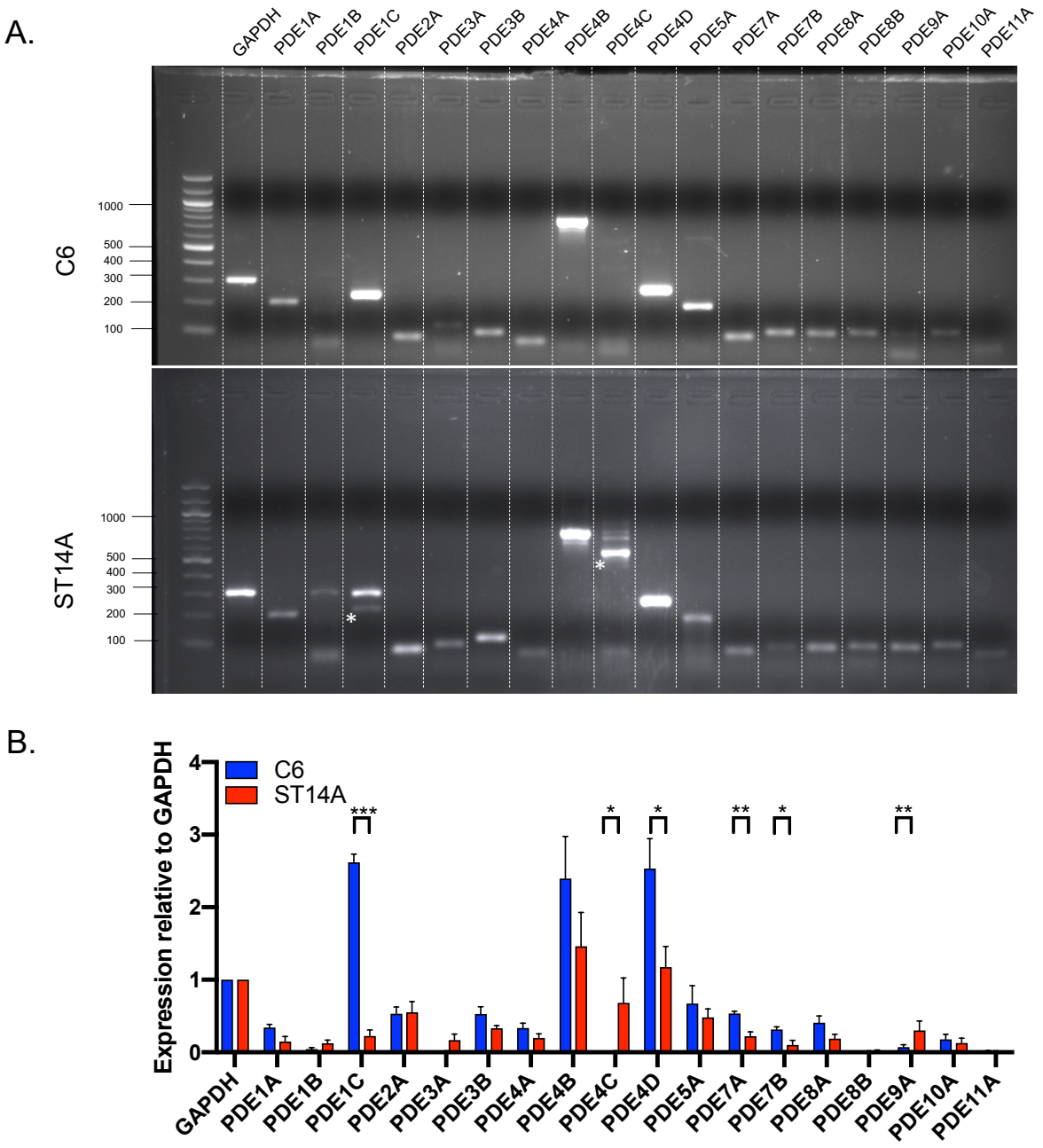

Fig. 2. Expression profile of PDE isoenzymes in C6 and ST14A cells. *A.* Representative gel documentation showing amplified PDEs genes from C6 and ST14A cell line. (*) on the gel showed correct band size. *B.* Semi-quantitative mRNA levels in C6 cells and ST14A cells. Expression of each gene of interest was normalised relative to GAPDH. Data are expressed as the mean ± SEM from 5-7 individual repeats. Data were determined as statistically different (*, $p<0.05$; **, $p<0.01$; ***,

$p<0.001$) compared to individual isoenzyme between both cell lines using Student's t-test analysis.

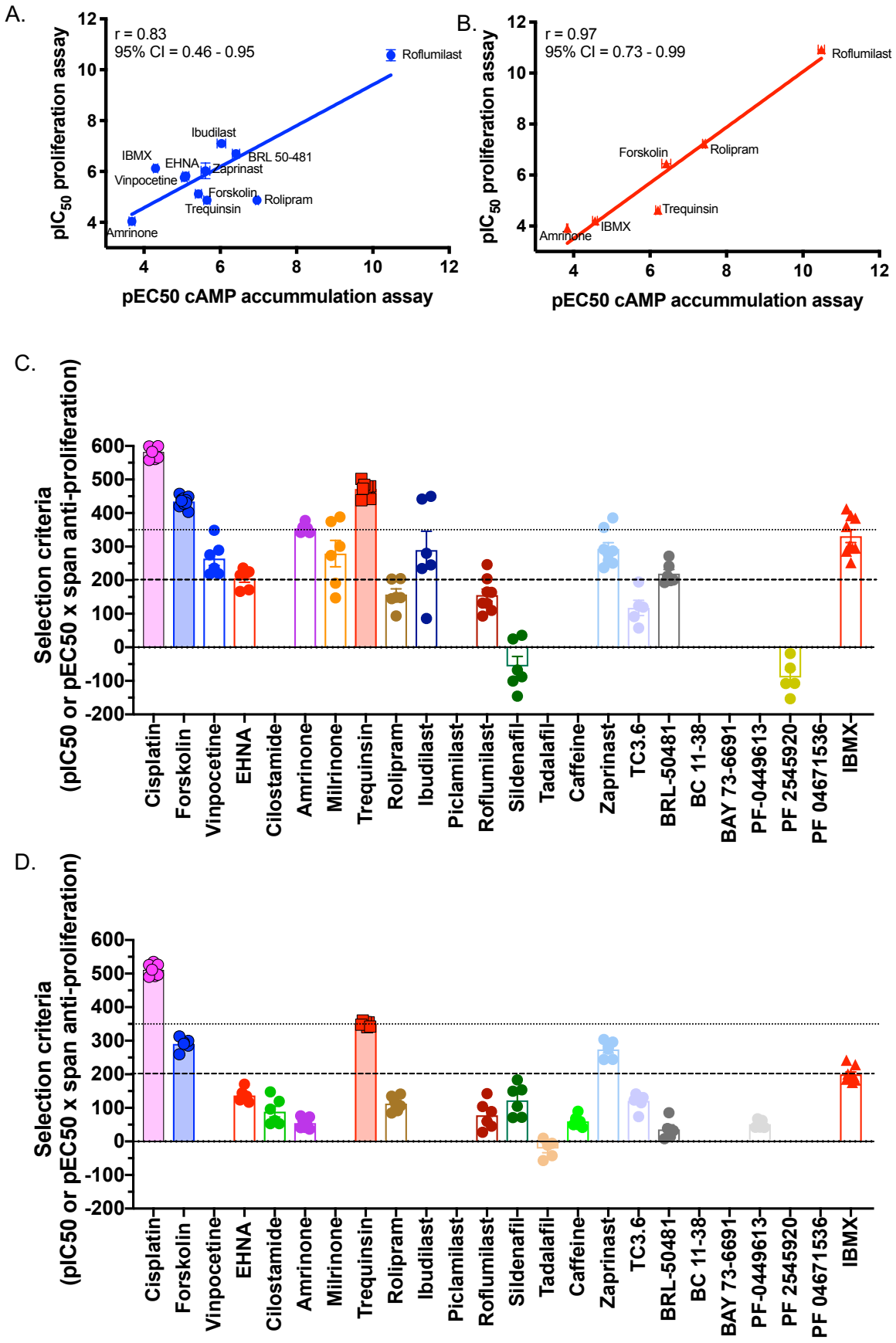
A.
r = 0.83
95% CI = 0.46 - 0.95
pIC50 proliferation assay
pEC50 cAMP accummulation assay
Roflumilast
Ibudilast
IBMX
EHNA
BRL 50-481
Zaprinast
Vinpocetine
Forskolin
Rolipram
Trequinsin
Amrinone
B.
r = 0.97
95% CI = 0.73 - 0.99
pIC50 proliferation assay
pEC50 cAMP accummulation assay
Roflumilast
Forskolin
Rolipram
Trequinsin
IBMX
Amrinone
C.
Selection criteria
(pIC50 or pEC50 x span anti-proliferation)
Cisplatin
Forskolin
Vinpocetine
EHNA
Cilostamide
Amrinone
Milrinone
Trequinsin
Rolipram
Ibudilast
Piclamilast
Roflumilast
Sildenafil
Tadalafil
Caffeine
Zaprinast
TC3.6
BRL-50481
BC 11-38
BAY 73-6691
PF-0449613
PF 2545920
PF 04671536
IBMX
D.
Selection criteria
(pIC50 or pEC50 x span anti-proliferation)
Cisplatin
Forskolin
Vinpocetine
EHNA
Cilostamide
Amrinone
Milrinone
Trequinsin
Rolipram
Ibudilast
Piclamilast
Roflumilast
Sildenafil
Tadalafil
Caffeine
Zaprinast
TC3.6
BRL-50481
BC 11-38
BAY 73-6691
PF-0449613
PF 2545920
PF 04671536
IBMX

Fig. 3. Elevation of intracellular cAMP is positively correlated with cell growth suppression. *A-B.* Correlation (with 95% confidence interval) of log potencies of each PDE inhibitor in C6 (A) and ST14A cells (B) was determined by calculating Pearson's correlation coefficient (r). *C-D.* Compound selection criteria from C6 (C) and ST14A cells (D) was calculated based on potency and efficacy in proliferation assay. The dashed lines represent threshold value of 200 (less stringent criteria) and the dotted lines a higher criteria value of 350. Individual data point was obtained from supplemental information (Fig. 1-4).

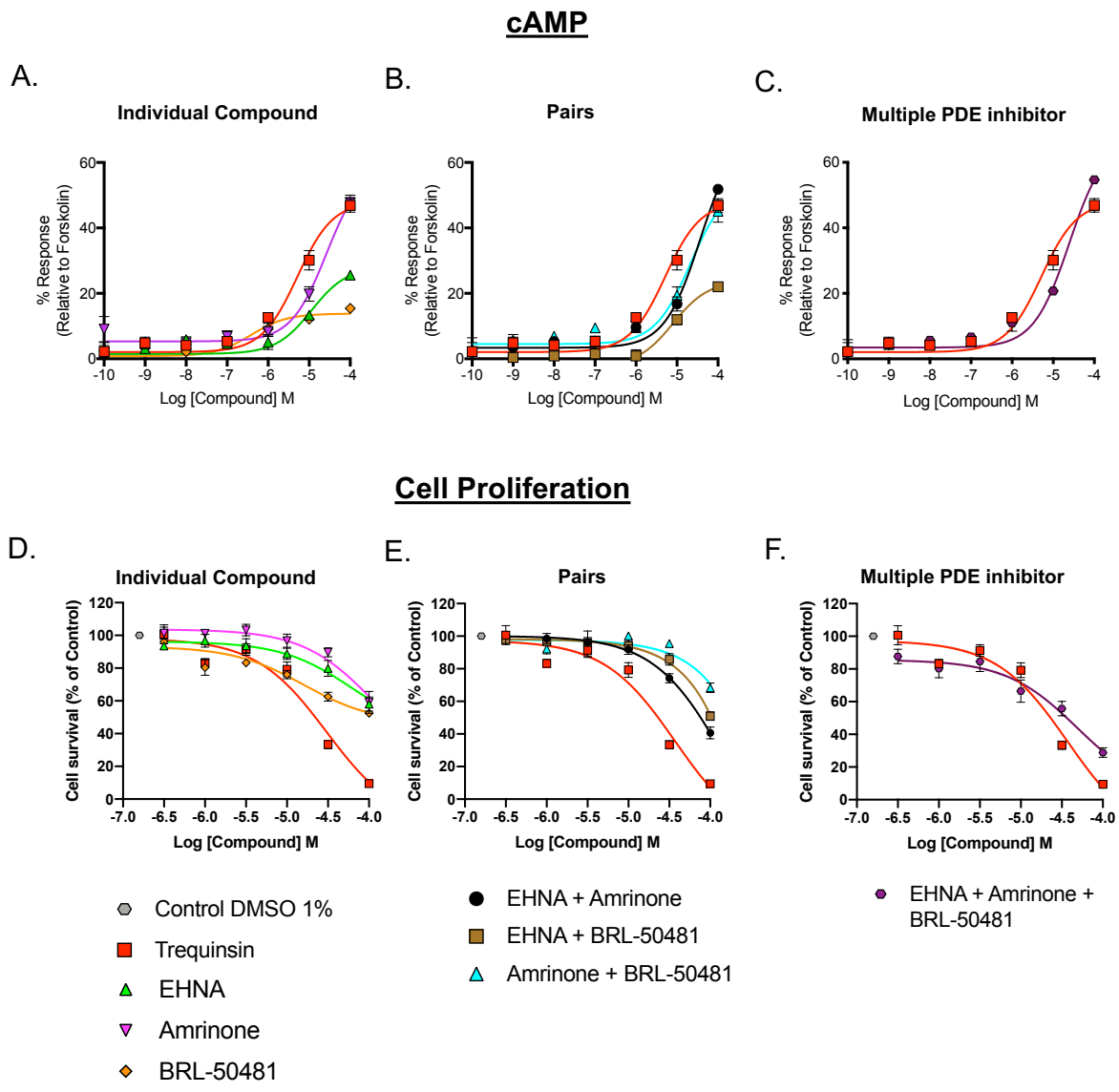

Fig. 4. The effect of selective PDE inhibitors, as individual, dual, or multiple treatments, on intracellular cAMP levels and cell proliferation in C6 glioma cells. *A-C.* cAMP accumulation was determined in C6 cells following 30 min stimulation with EHNA, Amrinone or BRL-50481 alone (A), in pairs (B), or combined (C). Data are expressed relative to 100 μM forskolin. *D-F.* Cell survival was determined in C6 cells following 72 hours incubation with EHNA, Amrinone or BRL-50481 alone (D), in pairs (E), or combined (F). Data are expressed as percentage of cell survival relative to vehicle from 6-9 data sets. The effect of trequinsin alone is displayed on each graph for comparison. All data are the mean ± SEM of 6–9 individual repeats.

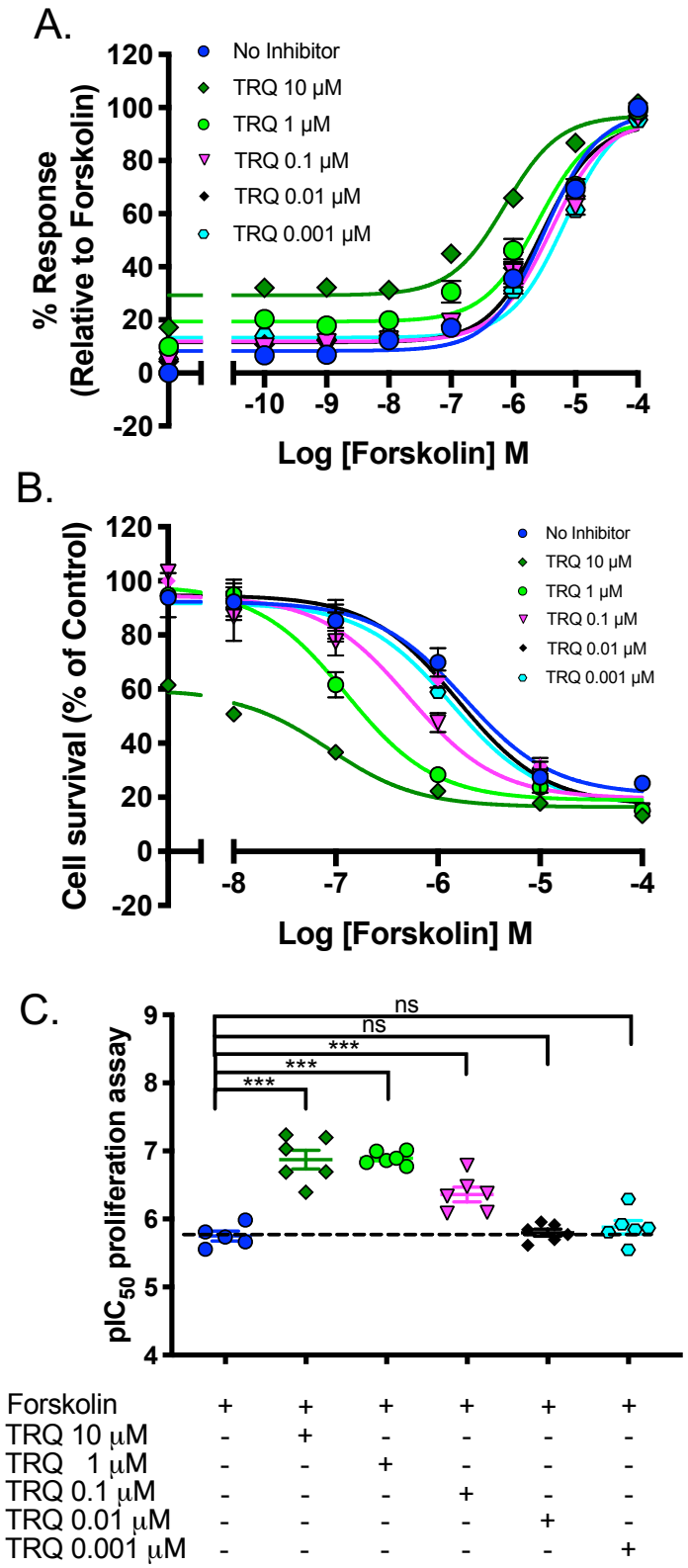

Fig. 5. Forskolin and trequinsin act synergistically to increase cAMP accumulation and suppress cell growth. *A*. Concentration-dependent effect of

trequinsin upon cAMP accumulation in C6 cells following 30 min stimulation with forskolin. Data are expressed relative to 100 μM forskolin in the absence of trequinsin. *B*. Concentration-dependent inhibitory effect of trequinsin on C6 cell growth following 72-hour incubation with forskolin. Data are expressed as percentage cell survival relative to vehicle. *C*. pIC_{50} values for individual cell survival curves for each treatment condition. All data are the mean ± SEM of 6-9 individual repeats. Data were determined as statistically different (ns, not significant; ***, $p<0.001$) compared to forskolin using one-way ANOVA followed by Dunnett's *post-hoc* analysis. TRQ – trequinsin.

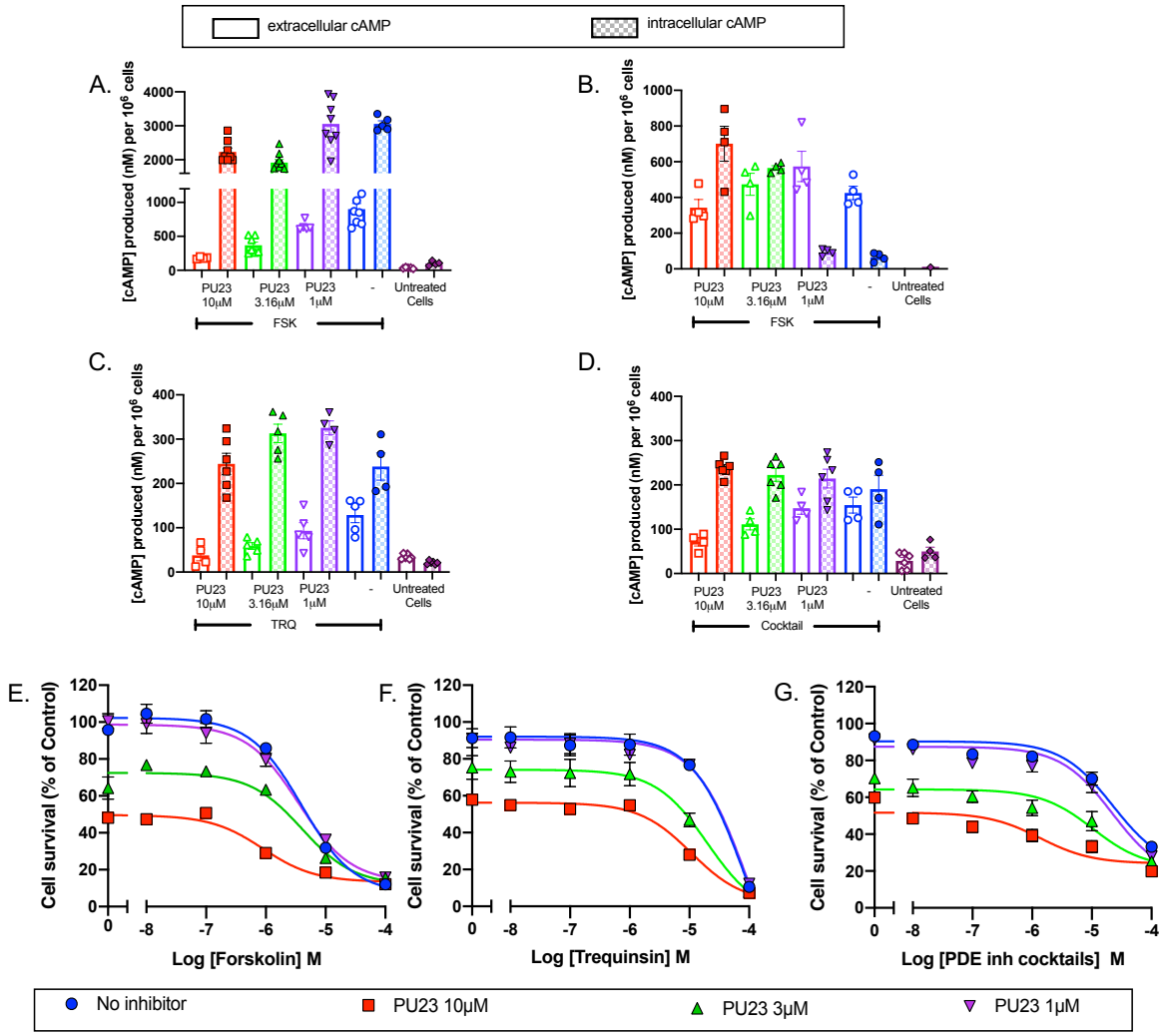

Fig.6. Elevation of intracellular cAMP by inhibiting its efflux is correlated with cell growth suppression in C6 cells. *A-D.* Extracellular and intracellular cAMP levels from C6 cells following stimulation with; forskolin for 1h (A) and 2h (B); trequinsin for 2h (C); or PDE inhibitor cocktail for 2h (D), in the presence and absence of a range of concentrations of the MRP4 inhibitor, PU23. *E-G.* Survival of C6 cells following 72-hour treatment with forskolin (E), trequinsin (F), or PDE inhibitor cocktail (G) in the absence and presence of increasing concentrations of PU23. Data are expressed as percentage cell survival relative to vehicle. All data are the mean ± SEM of 4-8 individual repeats. FSK – forskolin, TRQ – trequinsin.

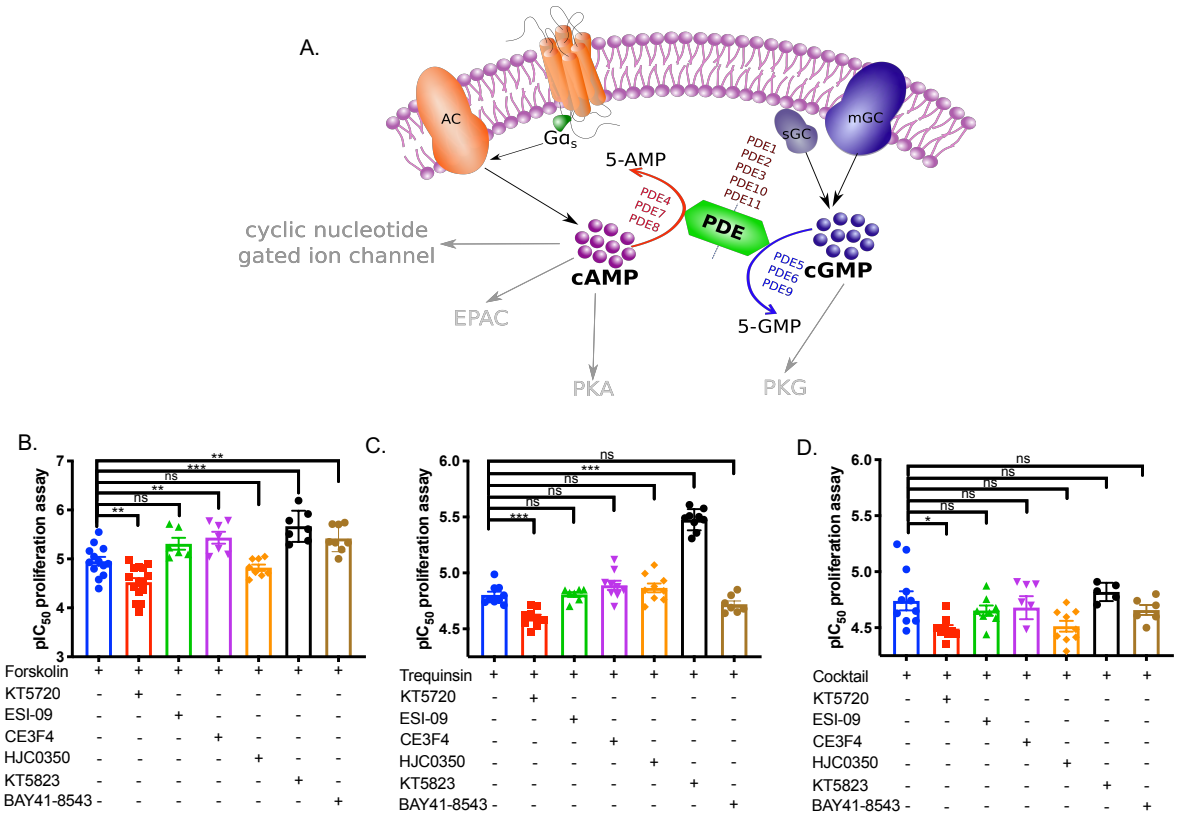

Fig. 7. The effect of downstream effectors of cAMP and cGMP on forskolin and trequinsin-mediated cell growth suppression of C6 cells. *A*. Schematic diagram illustrating cAMP and cGMP synthesis, degradation and downstream effectors. *B-D.* Cell survival was determined in C6 cells following 72 hours incubation with forskolin (B), trequinsin (C), or a combination of PDE2,3,7 inhibitors (D) in the presence either KT5720 (10 μM) , ESI-09 (10 μM), CE3F4 (10 μM), HJC0350 (10 μM), KT5823 (10 μM), BAY41-8543 (10 μM). Data are represented as individual pIC_{50} values for anti-proliferation curves for each treatment condition. Data were determined as statistically different (ns, not significant; *, $p< 0.05$; **, $p<0.01$; ***, $p<0.001$) compared to in the absence of compounds using one-way ANOVA followed by Dunnett's *post-hoc* analysis. KT5720 – PKA inhibitor, ESI-09 - non-selective Epac1/2 inhibitor, CE3F4 – Epac1 inhibitor, HJC0350 - Epac2 inhibitor, KT5823 PKG inhibitor, BAY41-8543 – GC activator.

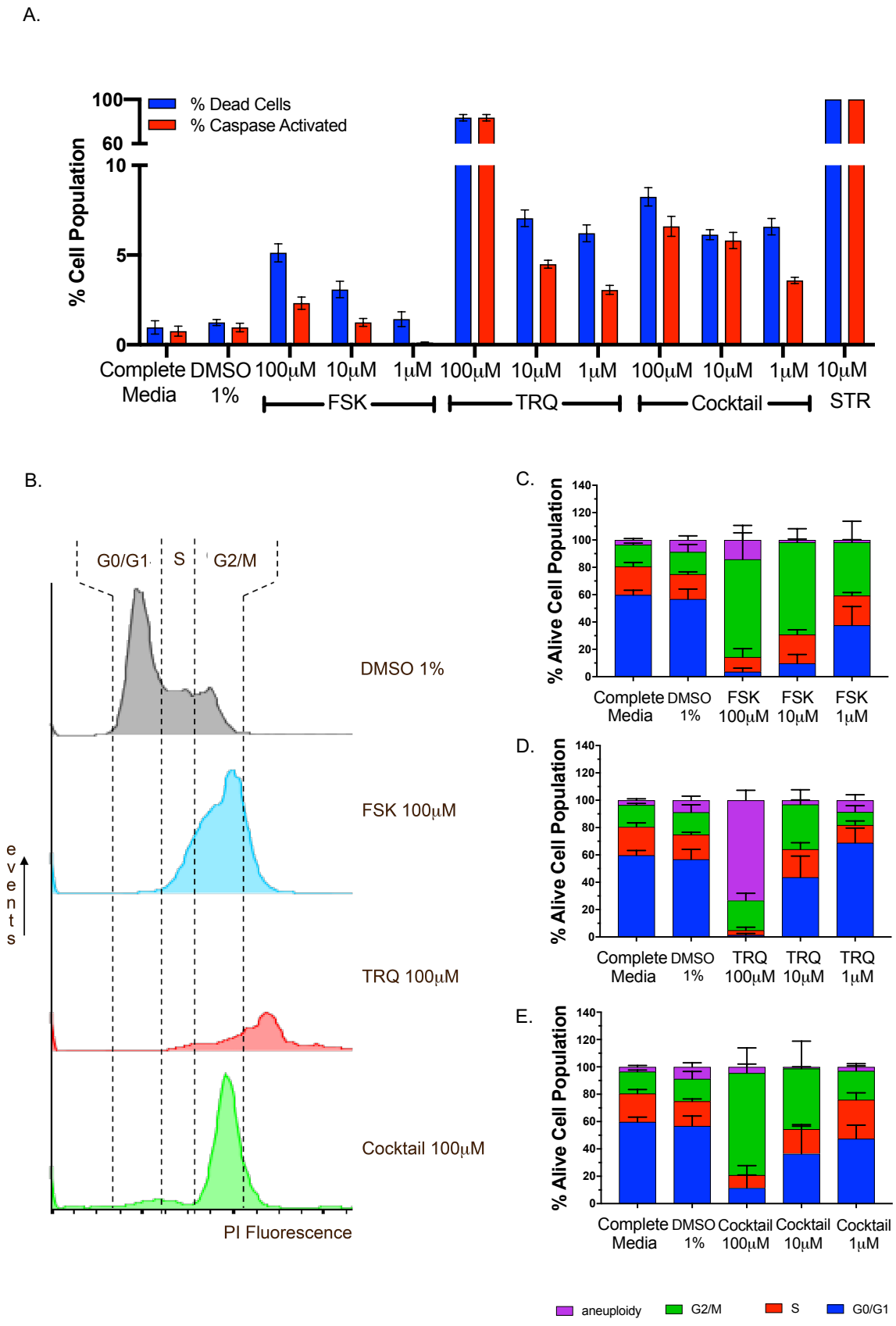

Fig. 8. Population of dead cells and activity of caspase-3/7 in C6 cells after 72 h treatment and cell cycle analysis by flow cytometry after PI staining. *A.*

Percentage of dead cells determined by staining with propidium iodide and the percentage of cells with activated caspase-3/7, visualised by CellEvent caspase-3/7. All values are normalised to total cell number in each well. Staurosporine 1 μM was used as a control for apoptotic cell death and cause 100% dead cells. *B.* Representative histograms of cell cycle distribution of C6 cells with selected treatment. *C-E*. Representative histograms of cells following treatment with forskolin (C), trequinsin (D), or PDE2,3,7 inhibitor cocktail (E) for 72 h. The percentage of cell distribution for each treatment including G_1, S, G_2/M, and dead cell population (n= 4-8 individual data). All data are the mean ± SEM of 5 individual repeats. Data were determined as statistically different (*, $p<0.05$; **, $p<0.01$; ***, $p<0.001$) compared to 1% DMSO using a one-way ANOVA followed by Dunnett's *post hoc* analysis. * $p<0.05$, ** $p<0.005$, *** $p<0.001$. FSK – forskolin, TRQ – trequinsin, STR – staurosporine.

Table 1.
Potency values for cAMP production (pEC_{50}) and for cell growth inhibition (pIC_{50}) of each PDE inhibitor in C6 glioma cells and ST14A cells.

Compounds	Target PDE(X) [∞]	C6				ST14A			
		pEC_{50}	**Span (cAMP)**	**pIC_{50}**	**Span (proliferation)**	**pEC_{50}**	**Span (cAMP)**	**pIC_{50}**	**Span (proliferation)**
Vinpocetine	1	5.10 ± 0.08*	27.86 ± 1.05***	5.83 ± 0.13*	45.33 ± 3.12***	4.16 ± 0.04***	13.15 ± 2.22***	N/A	N/A
EHNA	2	5.06 ± 0.07*	24.26 ± 1.78***	5.04 ± 0.25	36.34 ± 3.31***	N/A	N/A	6.57 ± 0.08***	20.86 ± 1.20***
Cilostamide	3	7.19 ± 0.09***	15.20 ± 1.45***	N/A	N/A	N/A	N/A	8.39 ± 0.15***	10.56 ± 1.90
Amrinone	3	3.68 ± 0.08***	108.9 ± 4.82***	4.11 ± 0.04***	86.44 ± 2.26	3.84 ± 0.02***	89.70 ± 1.12**	3.91 ± 0.11***	54.37 ± 6.17***
Milrinone	3	N/A	N/A	8.06 ± 0.13***	34.49 ± 4.66***	7.05 ± 0.18***	27.45 ± 2.35	N/A	N/A
Trequinsin	2,3,7	5.65 ± 0.08	50.57 ± 2.02***	4.87 ± 0.07	96.93 ± 0.94	6.21 ± 0.06	80.31 ± 1.85	4.62 ± 0.04***	75.82 ± 0.79***
Rolipram	4	6.96 ± 0.04***	60.46 ± 3.74	6.78 ± 0.20***	23.44 ± 2.94***	7.41 ± 0.04***	59.26 ± 4.11**	7.23 ± 0.05***	15.57 ± 1.28***
Ibudilast	4	6.03 ± 0.11***	64.21 ± 3.46	7.05 ± 0.17***	31.76 ± 1.30***	6.15 ± 0.12	48.64 ± 2.18***	N/A	N/A
Piclamilast	4	8.72 ± 0.04***	41.32 ± 2.87***	N/A	N/A	9.02 ± 0.14***	35.24 ± 1.96***	N/A	N/A
Roflumilast	4	10.47 ± 0.03***	54.58 ± 3.12	10.57 ± 0.22***	14.72 ± 1.66***	10.48 ± 0.08***	28.77 ± 0.78***	10.92 ± 0.09***	7.19 ± 1.63***
Sildenafil	5	N/A	N/A	8.56 ± 0.16***	-6.77 ± 3.54$^{***\#}$	8.79 ± 0.20***	-4.57 ± 0.93$^{***\#}$	9.67 ± 0.11***	12.71 ± 2.02***
Tadalafil	5	N/A	N/A	N/A	N/A	7.88 ± 0.04***	-23.15 ± 1.38$^{***\#}$	8.81 ± 0.43***	-2.69 ± 1.55$^{***\#}$
Caffeine	1,4,5	N/A	N/A	N/A	N/A	N/A	N/A	6.65 ± 0.06 ***	9.02 ± 1.08***
Zaprinast	5,6,9,11	5.61 ± 0.11	14.27 ± 1.12***	6.03 ± 0.30***	49.70 ± 4.60***	N/A	N/A	5.86 ± 0.09***	46.71 ± 1.45***
TC3.6	7	N/A	N/A	7.53 ± 0.26***	15.31 ± 2.47***	N/A	N/A	5.69 ± 0.05***	21.22 ± 1.49***
BRL-50481	7	6.41 ± 0.09***	31.3 ± 1.67***	6.70 ± 0.15 ***	33.07 ± 2.74***	N/A	N/A	7.73 ± 0.24***	4.52 ± 1.68***
BC 11-38	8	N/A	N/A	N/A	N/A	N/A	N/A	N/A	N/A
BAY-736691	9	N/A	N/A	N/A	N/A	N/A	N/A	N/A	N/A
PF-0449613	9	N/A	N/A	N/A	N/A	7.55 ± 0.12***	-23.48 ± 1.75$^{***\#}$	8.05 ± 0.08***	6.37 ± 0.72
PF 2545920	10A	N/A	N/A	9.46 ± 0.06***	-8.97 ± 3.05$^{\#}$	N/A	N/A	10.78 ± 0.11***	11.94 ± 4.13
PF 04671536	11	N/A	N/A	N/A	N/A	N/A	N/A	N/A	N/A
IBMX	Non-selective	4.30 ± 0.06***	42.79 ± 1.53***	6.12 ± 0.06***	54.17 ± 3.20	4.56 ± 0.06***	57.53 ± 3.52	4.20 ± 0.09	47.95 ± 2.70
Forskolin	AC activator	5.43 ± 0.08	64.97 ± 3.51	5.12 ± 0.06	84.70 ± 1.44	6.43 ± 0.12	74.06 ± 3.07	6.44 ± 0.02	45.11 ± 1.22
Cisplatin	DNA crosslinker	N/A	N/A	6.02 ± 0.09***	96.85 ± 2.57	N/A	N/A	5.92 ± 0.09***	86.50 ± 2.30***

N/A – not applicable; compounds did not have any effect on cAMP production or cell growth inhibition. [∞], unless mentioned, targets refer to particular PDE isoform. Data are presented as the mean ± SEM of 6-9 individual repeat. Data were determined as statistically different (*, $p<0.05$; ***, $p<0.001$) compared to forskolin using one-way ANOVA followed by Dunnett's *post-hoc* analysis. [#], showing negative responses, either suppressing cAMP accumulation or being proliferative.

Table 2.
Summary of the pharmacological effects of each PDE inhibitor on cAMP production and cell proliferation

Compound	Target	C6		ST14A	
		cAMP	Proliferation	cAMP	Proliferation
Vinpocetine	1	↑	↓↓	↑	-
EHNA	2	↑	↓↓	-	↓
Cilostamide	3	↑	-	-	↓
Amrinone	3	↑↑↑	↓↓↓	↑↑↑	↓↓↓
Milrinone	3	-	↓↓	↑	-
Trequinsin	2,3,7	↑↑↑	↓↓↓	↑↑↑	↓↓↓
Rolipram	4	↑↑↑	↓	↑↑↑	↓
Ibudilast	4	↑↑↑	↓↓	↑↑	-
Piclamilast	4	↑↑	-	↑↑	-
Roflumilast	4	↑↑↑	↓	↑	↓
Sildenafil	5	-	↑	↓	↓
Tadalafil	5	-	↑	↓	↑
Caffeine	1,4,5	Bell-shape	-	-	↓
Zaprinast	5,6,9,11	↑	↓↓	-	↓↓
TC3.6	7	-	↓	-	↓
BRL-50481	7	↑↑	↓↓	-	↓
BC 11-38	8	-	-	-	-
BAY-736691	9	-	-	-	-
PF-0449613	9	-	-	↓	↓
PF 2545920	10A	-	↑	-	↓
PF 04671536	11	-	-	-	-
IBMX	Non-selective	↑↑	↓↓↓	↑	↓↓

↑ = increase 10-30%, ↑↑ = increase 31-50%, ↑↑↑= increase >50%, ↓: suppress 10-30%, ↓↓: suppress 31-50%, ↓↓↓: suppress >50%

Table 3.
C6- proliferation assay-combinatorial effect of PDE2, 3, 7 inhibitors

Compound	cAMP accumulation assay		Proliferation Assay		Selection criteria*
	pEC_{50}	Span	pIC_{50}	Span	
Trequinsin	5.33 ± 0.11	46.31 ± 1.98	4.52 ± 0.11	91.21 ± 8.26	411.94 ± 38.52
EHNA	4.91 ± 0.10	26.19 ± 0.89	4.20 ± 0.21	57.21 ± 10.48	240.44 ± 45.57
Amrinone	4.58 ± 0.04	53.88 ± 1.63	3.94 ± 0.15	87.79 ± 13.62	346.01 ± 55.26
BRL-50481	6.20 ± 0.34	13.86 ± 0.74	4.79 ± 0.17	47.02 ± 4.45	225.39 ± 22.73
EHNA + amrinone	4.58 ± 0.03	62.51 ± 2.17	4.19 ± 0.17	85.97 ± 12.32	361.56 ± 53.66
EHNA + BRL-50481	5.05 ± 0.20	27.21 ± 1.40	4.07 ± 0.13	77.77 ± 9.73	316.34 ± 40.85
Amrinone + BRL-50481	4.65 ± 0.07	49.65 ± 2.95	3.77 ± 0.17	66.75 ± 11.94	248.98 ± 45.30
EHNA + amrinone + BRL-50481	4.58 ± 0.07	64.97 ± 1.82	4.52 ± 0.14	84.64 ± 8.69	382.12 ± 41.10

Data are expressed as mean ± SEM from 7-10 individual data.

* Compound selection criteria was calculated based on potency and efficacy in proliferation assay (data obtained from Figure 4).

Table 1.
Potency values for cAMP production (pEC_{50}) and for cell growth inhibition (pIC_{50}) of each PDE inhibitor in C6 glioma cells and ST14A cells.

Compounds	Target PDE(X) [∞]	C6				ST14A			
		pEC_{50}	**Span (cAMP)**	**pIC_{50}**	**Span (proliferation)**	**pEC_{50}**	**Span (cAMP)**	**pIC_{50}**	**Span (proliferation)**
Vinpocetine	1	5.10 ± 0.08*	27.86 ± 1.05***	5.83 ± 0.13*	45.33 ± 3.12***	4.16 ± 0.04***	13.15 ± 2.22***	N/A	N/A
EHNA	2	5.06 ± 0.07*	24.26 ± 1.78***	5.04 ± 0.25	36.34 ± 3.31***	N/A	N/A	6.57 ± 0.08***	20.86 ± 1.20***
Cilostamide	3	7.19 ± 0.09***	15.20 ± 1.45***	N/A	N/A	N/A	N/A	8.39 ± 0.15***	10.56 ± 1.90
Amrinone	3	3.68 ± 0.08***	108.9 ± 4.82***	4.11 ± 0.04***	86.44 ± 2.26	3.84 ± 0.02***	89.70 ± 1.12**	3.91 ± 0.11***	54.37 ± 6.17***
Milrinone	3	N/A	N/A	8.06 ± 0.13***	34.49 ± 4.66***	7.05 ± 0.18***	27.45 ± 2.35	N/A	N/A
Trequinsin	2,3,7	5.65 ± 0.08	50.57 ± 2.02***	4.87 ± 0.07	96.93 ± 0.94	6.21 ± 0.06	80.31 ± 1.85	4.62 ± 0.04***	75.82 ± 0.79***
Rolipram	4	6.96 ± 0.04***	60.46 ± 3.74	6.78 ± 0.20***	23.44 ± 2.94***	7.41 ± 0.04***	59.26 ± 4.11**	7.23 ± 0.05***	15.57 ± 1.28***
Ibudilast	4	6.03 ± 0.11***	64.21 ± 3.46	7.05 ± 0.17***	31.76 ± 1.30***	6.15 ± 0.12	48.64 ± 2.18***	N/A	N/A
Piclamilast	4	8.72 ± 0.04***	41.32 ± 2.87***	N/A	N/A	9.02 ± 0.14***	35.24 ± 1.96***	N/A	N/A
Roflumilast	4	10.47 ± 0.03***	54.58 ± 3.12	10.57 ± 0.22***	14.72 ± 1.66***	10.48 ± 0.08***	28.77 ± 0.78***	10.92 ± 0.09***	7.19 ± 1.63***
Sildenafil	5	N/A	N/A	8.56 ± 0.16***	-6.77 ± 3.54$^{***\#}$	8.79 ± 0.20***	-4.57 ± 0.93$^{***\#}$	9.67 ± 0.11***	12.71 ± 2.02***
Tadalafil	5	N/A	N/A	N/A	N/A	7.88 ± 0.04***	-23.15 ± 1.38$^{***\#}$	8.81 ± 0.43***	-2.69 ± 1.55$^{***\#}$
Caffeine	1,4,5	N/A	N/A	N/A	N/A	N/A	N/A	6.65 ± 0.06 ***	9.02 ± 1.08***
Zaprinast	5,6,9,11	5.61 ± 0.11	14.27 ± 1.12***	6.03 ± 0.30***	49.70 ± 4.60***	N/A	N/A	5.86 ± 0.09***	46.71 ± 1.45***
TC3.6	7	N/A	N/A	7.53 ± 0.26***	15.31 ± 2.47***	N/A	N/A	5.69 ± 0.05***	21.22 ± 1.49***
BRL-50481	7	6.41 ± 0.09***	31.3 ± 1.67***	6.70 ± 0.15 ***	33.07 ± 2.74***	N/A	N/A	7.73 ± 0.24***	4.52 ± 1.68***
BC 11-38	8	N/A	N/A	N/A	N/A	N/A	N/A	N/A	N/A
BAY-736691	9	N/A	N/A	N/A	N/A	N/A	N/A	N/A	N/A
PF-0449613	9	N/A	N/A	N/A	N/A	7.55 ± 0.12***	-23.48 ± 1.75$^{***\#}$	8.05 ± 0.08***	6.37 ± 0.72
PF 2545920	10A	N/A	N/A	9.46 ± 0.06***	-8.97 ± 3.05$^{\#}$	N/A	N/A	10.78 ± 0.11***	11.94 ± 4.13
PF 04671536	11	N/A	N/A	N/A	N/A	N/A	N/A	N/A	N/A
IBMX	Non-selective	4.30 ± 0.06***	42.79 ± 1.53***	6.12 ± 0.06***	54.17 ± 3.20	4.56 ± 0.06***	57.53 ± 3.52	4.20 ± 0.09	47.95 ± 2.70
Forskolin	AC activator	5.43 ± 0.08	64.97 ± 3.51	5.12 ± 0.06	84.70 ± 1.44	6.43 ± 0.12	74.06 ± 3.07	6.44 ± 0.02	45.11 ± 1.22
Cisplatin	DNA crosslinker	N/A	N/A	6.02 ± 0.09***	96.85 ± 2.57	N/A	N/A	5.92 ± 0.09***	86.50 ± 2.30***

N/A – not applicable; compounds did not have any effect on cAMP production or cell growth inhibition. [∞], unless mentioned, targets refer to particular PDE isoform. Data are presented as the mean ± SEM of 6-9 individual repeat. Data were determined as statistically different (*, $p<0.05$; ***, $p<0.001$) compared to forskolin using one-way ANOVA followed by Dunnett's *post-hoc* analysis. [#], showing negative responses, either suppressing cAMP accumulation or being proliferative.

Percentage of dead cells determined by staining with propidium iodide and the percentage of cells with activated caspase-3/7, visualised by CellEvent caspase-3/7. All values are normalised to total cell number in each well. Staurosporine 1 μM was used as a control for apoptotic cell death and cause 100% dead cells. *B.* Representative histograms of cell cycle distribution of C6 cells with selected treatment. *C-E*. Representative histograms of cells following treatment with forskolin (C), trequinsin (D), or PDE2,3,7 inhibitor cocktail (E) for 72 h. The percentage of cell distribution for each treatment including G_1, S, G_2/M, and dead cell population (n= 4-8 individual data). All data are the mean ± SEM of 5 individual repeats. Data were determined as statistically different (*, $p<0.05$; **, $p<0.01$; ***, $p<0.001$) compared to 1% DMSO using a one-way ANOVA followed by Dunnett's *post hoc* analysis. * $p<0.05$, ** $p<0.005$, *** $p<0.001$. FSK – forskolin, TRQ – trequinsin, STR – staurosporine.